AD_____

Award Number: W81XWH-07-2-0028

TITLE: Interferon Antagonism as a Common Virulence Factor of Hemorrhagic Fever Viruses

PRINCIPAL INVESTIGATOR: Adolfo Garcia Sastre, Ph.D.
Connie S. Schmaljohn, Ph.D.

CONTRACTING ORGANIZATION: Mount Sinai Medical Center
New York, NY 10029

REPORT DATE: February 2008

TYPE OF REPORT: Annual

PREPARED FOR: U.S. Army Medical Research and Materiel Command
Fort Detrick, Maryland 21702-5012

REPORT DOCUMENTATION PAGE

Form Approved
OMB No. 0704-0188

1. REPORT DATE *(DD-MM-YYYY)*	**2. REPORT TYPE**	**3. DATES COVERED** *(From - To)*
01-02-2008	Annual	25 JAN 2007-24 JAN 2008

4. TITLE AND SUBTITLE

Interferon Antagonism as a Common Virulence Factor of Hemorrhagic Fever Viruses

5a. CONTRACT NUMBER

5b. GRANT NUMBER
W81XWH-07-2-0028

5c. PROGRAM ELEMENT NUMBER

6. AUTHOR(S)
Adolfo Garcia Sastre, Ph.D.; Connie S. Schmaljohn, Ph.D.

E-Mail: connie.schmaljohn@amedd.army.mil

5d. PROJECT NUMBER

5e. TASK NUMBER

5f. WORK UNIT NUMBER

7. PERFORMING ORGANIZATION NAME(S) AND ADDRESS(ES)

Mt. Sinai School of Medicine
New York, NY 10029

8. PERFORMING ORGANIZATION REPORT NUMBER

9. SPONSORING / MONITORING AGENCY NAME(S) AND ADDRESS(ES)
U.S. Army Medical Research and Materiel Command
Fort Detrick, Maryland 21702-5012

10. SPONSOR/MONITOR'S ACRONYM(S)

11. SPONSOR/MONITOR'S REPORT NUMBER(S)

12. DISTRIBUTION / AVAILABILITY STATEMENT
Approved for Public Release; Distribution Unlimited

13. SUPPLEMENTARY NOTES

14. ABSTRACT
We examined the ability of viruses in the Hantavirus and Nairovirus genera of the family Bunyaviridae to interfere with host signaling pathways involved in innate immunity. For the nairovirus, Crimean Congo hemorrhagic fever virus (CCHFV), we found that the viral polymerase gene contains a predicted ovarian tumor (OTU) protease domain that functions to deconjugate ubiquitin and interferon stimulated gene product 15 (ISG15) from host proteins. Both ubiquitin and ISG15 reversibly conjugate to proteins via a conserved LRLRGG C-terminal motif, mediating important innate antiviral responses. We showed that the OTU domain-containing proteases of CCHFV hydrolyzes ubiquitin and ISG15 from many cellular target proteins. This broad activity contrasts with the target specificity of known mammalian OTU domain-containing proteins. The biological significance of this activity of viral OTU domain-containing proteases was evidenced by their capacity to inhibit nuclear factor kappa B (NF-κB) dependent signaling and to antagonize the antiviral effects of ISG15. The deconjugating activity of viral OTU proteases represents a novel viral immune evasion mechanism that inhibits ubiquitin- and ISG15-dependent antiviral pathways. For the hantavirus, Hantaan virus (HTNV), we found that the nucleocapsid protein was able to inhibit tumor necrosis factor alpha (TNF-α)-induced activation of NF-κB as measured by a reporter assay and activation of endogenous p65, a NF-κB subunit. We showed an interaction between HTNV N protein and importin-α, a nuclear import molecule responsible for shuttling NF-κB to the nucleus. These data suggest that HTNV N protein can sequester NF-κB in the cytoplasm, thus inhibiting its activity.

15. SUBJECT TERMS
Hemorrhagic fever viruses; Innate immunity; interferon antagonism, NF-κB; TNF-α

16. SECURITY CLASSIFICATION OF:			**17. LIMITATION OF ABSTRACT**	**18. NUMBER OF PAGES**	**19a. NAME OF RESPONSIBLE PERSON**
a. REPORT	**b. ABSTRACT**	**c. THIS PAGE**			USAMRMC
U	U	U	UU	33	**19b. TELEPHONE NUMBER** *(include area code)*

Table of Contents

INTRODUCTION: The overarching goal of this project is to identify common mechanisms that hemorrhagic fever viruses use to evade host innate immune responses and to develop means to overcome those evasion strategies. Among the viruses in our study are representatives of three different genera of the family *Bunyaviridae*: Hantaan (HTNV), Rift Valley fever (RVFV), and Crimean Congo hemorrhagic fever (CCHFV). In addition, we are studying members of the *Filoviridae* and *Arenaviridae* families: Ebola virus (EBOV) and Lassa virus (LASV), respectively. Our approach and goals are to (1) determine if the viruses evade host innate immunity; (2) to identify viral genes and proteins involved in immune evasion; (3) elucidate the mechanism(s) by which evasion occurs; and, (4) search for therapeutics that are not susceptible to those mechanisms. Studies from the first year centered on CCHFV and hantaviruses. These viruses have three-segmented RNA genomes (S, M, L), which encode the nucleocapsid N protein, glycoproteins (Gn and Gc), and the transcriptional polymerase (L), respectively in the virus complementary RNA. Our studies indicate that the L segment of CCHFV and the S segment of hantaviruses are used in infected cells to evade host innate immunity through novel and previously unknown mechanisms of action.

BODY OF REPORT:

CCHFV possesses a novel evasion strategy that is mediated by the viral polymerase gene

We identified a unique domain in the polymerase gene of CCHFV that has ubiquitin deconjugating activity. As ubiquitination is a key factor in signaling transcription factors needed to trigger innate immunity, the presence of this domain allows CCHFV to interfere with the induction of at least one pathway in the host response to viral infection. The results of that study were published (manuscript is appended), and detailed methods and specific results are presented therein. As described in the manuscript, we showed that a viral ovarian tumor (OTU) domain is present in the L gene of CCHFV and that it functions as a protease able to hydrolyze ubiquitin and interferon stimulating gene product 15 (ISG15) from conjugated proteins. This protease activity provides the physiologic capacity to evade two different cytokine pathways, IFN$\alpha\beta$ and TNFα, which are fundamentally important for innate immunity. Viral OTU domain proteases inhibit protein ISGylation in order to counter some of IFN$\alpha\beta$'s antiviral effects, while viral deubiquitinating activity prevents TNF-α transcriptional effects. This dual deconjugating activity provides an elegant example of the economy of viral evolution since both ubiquitin and ISG15 rely on a conserved LRLRGG motif that is essential for their conjugation. By targeting this conjugation process, viruses can evade or subvert many different cellular processes.

Although OTU domains are present in mammalian proteins, we found that the OTU domain-containing cellular proteins A20, Cezanne, Otubain 1, Otubain 2 and VCIP do not exhibit the unique capacity of the CCHFV OTU domain protease to target both ubiquitin and ISG15 conjugates. We speculate that other viral proteases, perhaps including some that do not have clear OTU domains, will be found to target both ubiquitin and ISG15 dependent processes. We further speculate that the OTU domain specificity and deconjugating activity provides a unique target for antiviral drug development. The characterization of the CCHFV-L OTU domain and the development of in vitro assays for its enzymatic activities as described in this study will make it feasible to screen for potential inhibitors specific for CCHFV-L and other OTU domain-containing viral proteins.

Hantaan virus (HTNV) nucleocapsid (N) protein interferes with tumor necrosis factor alpha (TNF-α)-signaling for the induction of the NF-κB.

The results, as described below, are currently being reviewed internally for submission to J. Virology.

TNF-α is a major proinflammatory cytokine produced by a variety of cell types that include macrophages, endothelial cells and epithelial cells and the receptor is constitutively expressed on most cell types (26). TNF-α is pleiotropic and can regulate the response of immune cells as well as induce inflammation, differentiation, apoptosis, and is involved in protecting the host from pathogen infections. Upon TNF-α ligand binding, TNF-associated death domain (TRADD) associates with the TNF receptors (TNFR) and serves as an adaptor molecule that recruits TNFR-associated factor-2 (TRAF-2) and receptor interacting protein (RIP) (10). This complex of proteins leads to the activation of kinases that phosphorylate inhibitor of κB (IκB) (10). The ubiquitin-proteosome pathway initiates degradation of IκB allowing for NF-κB dimers to translocate to the nucleus and regulate transcription of its target genes.

NF-κB transcription factors are dimers composed of five subunits belonging to the Rel family (20). The five subunits of p65 (Rel A), Rel B, c-Rel, p50, and p52 can form various dimers (2, 23, 24). The p50/p65 heterodimers are the best characterized and are the most abundant form of the NF-κB transcription factors in most cell types (8). IκB is responsible for sequestering NF-κB in the cytoplasm by masking its nuclear localization signal (NLS) (3, 6, 9, 27). Proteins that require nuclear translocation contain a NLS and are transported by importin α via its' interaction with the cargo's NLS (7, 16). To date there have been six importin α family members identified (importin α1-6), all of which carry various cargo, including signal transducers and activators of trancription (STATs) and NF-κB (4, 11, 12, 17, 21). Importantly, it was recently reported that TNF-α-induced nuclear localization of p50/p65 heterodimers is mediated by importin α3 and importin α4 (5). However, there have also been reports of importin α1 and importin α2 interacting with NF-κB, but their role in transport and activation remains unclear (5). Because of the multifaceted nature of TNF-α and NF-κB, the NF-κB subunits and the importin α proteins have become prime targets of viruses to evade the outcome of inflammatory pathways.

Hantaviruses can cause two distinct types of human disease: hemorrhagic fever with renal syndrome (HFRS) and hantavirus pulmonary syndrome (HPS) (19). Hantavirus associated diseases are thought to be immunologically mediated and there have been numerous reports of patients having elevated plasma levels of TNF-α during the acute phase of HFRS (13-15). TNF-α positive cells can also be found in kidney and lung biopsies of HFRS and HPS patients. Clinically, hypotension and patient outcomes correlate with the levels of TNF-α (14, 15).

Recently, studies, in addition to ours, suggest that hantaviruses can subvert innate immunity through several mechanisms. The Gc protein of the HPS-causing viruses, Andes virus (ANDV) and NY-1 virus (NY-1V) can inhibit activation of two important innate immune pathways, double stranded RNA (dsRNA) and interferon (IFN). NY-1V Gc has been shown to antagonize the activation of RIG-I, a protein involved in the induction of IFN (1). ANDV Gc can inhibit the phosphorylation of transcription factors STAT1 and STAT2 and this was also shown in HTNV infected cells (22). Furthermore, another HPS-causing hantavirus, Sin nombre virus, was also unable to induce production of IFN-α/β during infection (18). Considering the clinical relevance of TNF-α during infection, we sought to determine if HTNV might also interfere with this inflammatory pathway.

HTNV N protein inhibits TNFα-induced activation of NF-κB. To date there have been no reports of studies examining the ability of HTNV to antagonize the TNF-α signaling pathway. To determine if the HTNV N, Gn, or Gc proteins could inhibit TNF-α-induced activation of NF-κB, a human NF-κB promoter that transcriptionally regulates the expression of GFP was used as a reporter. No GFP was detected in any of the samples that were left untreated indicating that the conditions of our experiment alone, including the presence of viral proteins, could not induce activation of NF-κB (Fig. 1A and B). HTNV N protein was able to inhibit transcriptional GFP expression from the NF-κB responsive promoter at all concentrations of TNF-α when compared to empty vector (Fig 1A). HTNV glycoproteins only had little effect on GFP expression suggesting that this phenomenon is N protein specific (Fig. 1A). This inhibition occurred in a dose dependent manner but was still significantly less than the control empty vector (Fig 1A).

Proteosomal degradation of IκBα is required for the activation of NF-κB in the TNF-α pathway. In order to validate our assay, the proteosomal inhibitor MG132 was included as a control because it has been previously shown to inhibit this pathway. MG132 was also able to dramatically decrease the amount of GFP present in TNF-α treated cells and this was comparable to what we observed in cells expressing the HTNV S segment cDNA (Fig. 1A).

We also examined whether TNF-α-induced activation of our reporter system correlated with the amount of viral protein or MG132 present in cells. As expected, increasing amounts of empty vector and HTNV glycoproteins had no effect on the expression of the NF-kB-GFP reporter (Fig. 1B). However, inhibition of NF-kB- GFP was directly proportional to the amount of HTNV nucleocapsid and MG132 in cells, hence the greatest inhibition was observed with maximal N protein and MG132 present (Fig. 1B). It should also be noted that expression of

the HTNV N and glycoprotein genes were not adversely affected by the amount or time that cells were treated with TNF-α (data not shown).

HTNV N protein inhibits activation of endogenous NF-κB p50 and p65. In order to validate the NF-κB reporter assay used above, we next examined whether HTNV N protein was able to inhibit activation of endogenous p50 and p65 subunits, the most abundant of the heterodimers used as an NF-kB transcription factor. To quantify NF-kB transcription factor activation, we employed an ELISA that measures binding to NF-kB consensus oligonucleotide sequences, followed by detection of p50 and p65 subunits with antibodies. As expected, there was little activation of transfected and untreated cells indicating that viral gene expression and transfection alone could not activate NF-kB proteins (Fig. 2A). In contrast, similar levels of activated p50 and p65 were detected from nuclear extracts of TNF-α stimulated cells that were transfected with empty vector or HTNV-M cDNA (Fig 2A). Transfecting with HTNV -S cDNA significantly inhibited activation of p50 and p65 as determined with extracts of TNF-α stimulated cells and this was similar to what we observed with MG132 treated cells as compared to cells transfected with the empty vector (Fig. 2A). Although there was a small increase in activation of p50 and p65 in HTNV-S expressing cells treated with TNF-α as compared to untreated cells, this can most likely be explained by the fact that we were measuring activation of endogenous NF-kB in a total cell population, but not every cell was expressing the HTNV genes during the period of assay.

To confirm that cells were expressing viral genes, we prepared cytoplasmic extracts and examined them by immunoblotting to detect N protein (Fig. 2B) or by immunofluorescent antibody staining to detect Gn and Gc (Fig. 3). Levels of the housekeeping protein GAPDH were also measured to rule out the possibility that the decreased inhibition we observed for HTNV N protein and MG132 treatment was not due to differences in the amount of lysate used in our assay (Fig. 2B).

HTNV nucleocapsid inhibits TNF-α -induced nuclear translocation of NF-κB p65. The transcription factor ELISA used above is not able to distinguish between inhibition due to reduced DNA binding or to the inability of NF-kB to enter the nucleus. To test whether cellular localization was altered in TNF-α-treated cells expressing HTNV -S, we performed an immunofluorescence assay. When localization and expression of p65 was examined by microscopy, all unstimulated and transfected or MG 132-treated cells had the expected cytoplasmic localization with no apparent differences in p65 protein expression within cells (Fig 3, upper panel). In contrast, nuclear translocation of p65 was observed in cells transfected with empty vector or HTNV-M cDNA and treated with TNF-α (Fig. 3, lower panel, 1st and 3rd column). This indicates that there was no defect in the ability of p65 to move to the nucleus nor could transfection and viral gene expression alone inhibit this event. In contrast, TNF-α cells that were expressing HTNV-S cDNA had markedly reduced p65 that translocated to the nucleus (Fig. 3, lower panel, 2nd column). As expected, treatment of cells with MG132 was also able to inhibit p65 from entering the nucleus (Fig. 3, lower panel, 4th column). These data suggest that p65 is being sequestered in the cytoplasm by HTNV-N protein.

HTNV–S expression does not affect protein levels of p50 and p65 or degradation of IκB. Since it was difficult to definitively determine by microscopy whether the decreased nuclear p65 observed was due to retention in the cytoplasm or a decrease in the amount of total p65 present in cells expressing HTNV-S, we performed western blot analysis. No difference in the protein levels of p50 and p65 were observed in any of the samples that were transfected and unstimulated or stimulated with TNF-α (Fig. 4). This indicates that the observed decrease in nuclear localization of p65 was probably due to the inability of NF-κB to enter the nucleus. β-Actin was used as a control to ensure equal loading of samples.

The TNF-α pathway requires the association of numerous signaling molecules such as TRADD, TRAF-2, and RIP and alteration of any of these molecules could inhibit activation of NF-κB (25). The next question we wanted to address was whether the NF-κB proteins were being targeted directly by HTNV N protein or if a signaling molecule further upstream was being inhibited thus preventing activation of NF-κB. Since IκBα serves as an inhibitor of NF-κB and its degradation is required for translocation of activated NF-κB to the nucleus, we examined the ability of HTNV N protein to inhibit degradation of IκBα in the presence of TNF-α. Western blot analysis of IκBα levels demonstrated that TNF-α treatment was effective in subsequent

degradation of IκBα in all transfected samples including HTNV–S segment expressing cells (Fig 4). Furthermore, IκBα levels were similar in all unstimulated and transfected samples (Fig 4).

HTNV N protein binds to nuclear import proteins, importin α. The above data suggest that NF-κB is being directly sequestered by HTNV N protein or has lost its ability to translocate to the nucleus. To examine if NF-κB was directly targeted we performed co-immunoprecipitation experiments to determine if HTNV N protein could interact with p50 or p65. No interaction was detected between HTNV N protein and NF-κB proteins nor did we detect any inhibition of the phosphorylation of NF-κB in the presence of HTNV N protein when treated with TNF-α (data not shown). These results suggest that transport of NF-κB was likely inhibited by HTNV N protein.

It has been reported that NF-κB accumulates in the nucleus via interaction of importin α3 and importin α4 and its nuclear localization signal. We next wanted to ask whether HTNV nucleocapsid could interact with these or possibly other importin α molecules. FLAG-tagged importin α1, importin α2, importin α3, or importin α4 were co-transfected with empty or HTNV-S expression plasmids. Immunoprecipitation with an anti-HTNV-N protein polyclonal antibody followed by western blotting with anti-FLAG antibody was used to detect importin α proteins. The results indicate that HTNV N protein is able to interact with importin α1, importin α2, and importin α3 and that the presence of TNF-α is not required for this interaction (Fig. 5). Western blotting of whole cell lysates demonstrated that there were similar levels of importin α and nucleocapsid protein in our samples.

HTNV inhibits TNF-α-induced nuclear localization of NF-κB p65 without affecting IκBα degradation. The HTNV S segment transfection experiments clearly demonstrated inhibition of NF-κB. To confirm that infection with HTNV also inhibits TNF-α-induced activation of NF-κB by preventing nuclear localization, we examined virus infected cells by immunofluorescent antibody staining with antibodies to p65 and HTNV N protein. We did not detect nuclear p65 in unstimulated cells that were mock-infected or infected with HTNV (Fig. 6A, upper panel). As expected, TNF-α stimulated mock-infected cells had predominantly nuclear localization of p65 (Fig 6A, lower panel, 1st column). Interestingly, as infection progressed to day 5, the staining pattern of p65 became predominantly cytoplasmic in TNF-α treated cells and this was similar to that of unstimulated cells (Fig 6A, lower panel, 2nd column).

To confirm that there was no decrease in the total protein levels of p50 or p65 and that no upstream signaling molecules were being targeted, we performed western blot analysis. Mock-infected or HTNV-infected lysates harvested after unstimulation or stimulation with TNF-α had no apparent differences in the overall levels of p50 or p65, indicating that this was not the cause of decreased nuclear localization in the presence of virus (Fig 6B). HTNV was also unable to inhibit degradation of IκBα after being treated with TNF-α, suggesting that IκBα itself and signaling molecules upstream are not being targeted by HTNV (Fig. 6B).

Preliminary results:

In addition to the results described above, we also began studies to define other innate immune evasion strategies. We focused on antagonism of the Type 1 interferon (IFN) system because it is usually the first line of defense against viral infections. Evasion of the IFN response by viruses can occur by preventing IFN release, inhibiting IFN-signaling and/or activity of IFN stimulated genes. To date there have been no reports of studies examining IFN antagonism of hantaviruses or of CCHFV. To examine this for hantaviruses, lung epithelial cells (A549) were mock-infected or infected with the HPS-causing hantavirus, Andes virus (ANDV), for 7 days and left untreated or treated with IFN every day. We determined by Real Time RT-PCR and western blot that the ANDV S segment synthesis and nucleocapsid production peak on day 4. We also examined the levels of phosphorylated STAT1 and STAT2 by western blot. In infected samples left untreated, little phosphorylated STAT1 and STAT2 was detected up to 4 days post infection. Beyond 4 days post infection, phosphorylated STATs were not detectable by western blot and immunofluorescence. In samples treated with IFN, ANDV was able to inhibit phosphorylation of STAT1 and STAT2 to the greatest extent starting on day 3 when compared to mock-infected cells. Furthermore, this inhibition was not a result of STAT1 or STAT2 being degraded. These data suggest that hantaviruses have the capability to subvert a host IFN response.

To examine IFN antagonism with CCHFV, 293T or HepG2 cells were mock-infected or infected with CCHFV for 5 days and left untreated or treated with IFN every day. We found that CCHFV activates the transcription factor IRF-3, thus allowing for transcription and production of IFN. The IFN made during infection retains its ability to activate STATs through the IFN signaling pathway and allows for upregulation of IFN stimulated genes. We did not detect any degradation of PKR, eIF2-alpha, or ISG15, all of which are upregulated by IFN. These results have led to examination of other arms of the innate immune and proinflammatory responses that could be inhibited.

KEY RESEARCH ACCOMPLISHMENTS:

- CCHFV possesses a novel evasion strategy that is mediated by the viral polymerase gene and results in deconjugation of ubiquitin and ISG15 from host proteins.
- HTNV nucleocapsid protein interferes with tumor necrosis factor alpha (TNF-α)-signaling for the induction of the NF-κB by binding to cellular transport proteins and preventing their use in moving TNF-α from the cytoplasm to the nucleus of infected cells.

REPORTABLE OUTCOMES:

1. Frias-Staheli, N., N. V. Giannakopoulos, M. Kikkert, S. L. Taylor, A. Bridgen, J. Paragas, J. A. Richt, R. R. Rowland, C. S. Schmaljohn, D. J. Lenschow, E. J. Snijder, A. Garcia-Sastre, and H. W. Virgin. 2007. Ovarian tumor domain-containing viral proteases evade ubiquitin- and ISG15-dependent innate immune responses. Cell Host Microbe 2:404-16.

2. Taylor, S. L., Firas-Staheli, N., Garcia-Sastre, A., and Schmaljohn, C.S. Hantaan virus nucleocapsid protein binds to importin α proteins and inhibits tumor necrosis factor-α -induced activation of nuclear factor kappa-b. Manuscript in preparation.

CONCLUSION:

We discovered two previously unknown mechanisms that hemorrhagic fever viruses use to subvert innate immunity by disrupting NF-κB signaling pathways. For CCHFV, we discovered a domain in the viral polymerase protein with the capacity to inhibit NF-κB-dependent signaling (ubiquitination) and to antagonize the antiviral effects of ISG15 in vivo. For HTNV we showed that the viral nucleocapsid protein binds to cellular transport molecules (importins), preventing the transport of TNF-α into the host cell nucleus. By sequestering TNF-α in the cytoplasm, HTNV prevents its use as a transcription factor to stimulate host genes involved in inflammatory and apoptosis processes. This is especially important since elevated levels of TNF-α are a hallmark of hantaviral diseases. We suspect that the ability of HTNV N protein to bind to cellular importins relates to a specific region of the gene that encodes a nuclear localization signal (NLS). We observed that similar or identical NLS sequences are present in the N genes of other hantaviruses, thus we are currently performing additional studies to determine if this is a common mechanism used by HFRS and HPS causing hantaviruses, and perhaps by other hemorrhagic fever causing viruses as well. In addition to these two new discoveries, we also demonstrated that the hantavirus, Andes virus, interfere with the in JAK-STAT pathway of interferon induction by inhibiting translocation of STAT1 and STAT2 to the nucleus.

In summary, we made new discoveries concerning how hemorrhagic fever viruses are able to evade host innate immunity. Further studies are needed to determine if these mechanisms are common to several viruses and if they can be overcome by exogenous interferon or other therapeutic means.

REFERENCES: List all references pertinent to the report using a standard journal format (i.e. format used in *Science, Military Medicine*, etc.).

1. **Alff, P. J., I. N. Gavrilovskaya, E. Gorbunova, K. Endriss, Y. Chong, E. Geimonen, N. Sen, N. C. Reich, and E. R. Mackow.** 2006. The pathogenic NY-1 hantavirus G1 cytoplasmic tail inhibits RIG-I- and TBK-1-directed interferon responses. J Virol **80:**9676-86.
2. **Baeuerle, P. A., and D. Baltimore.** 1996. NF-kappa B: ten years after. Cell **87:**13-20.
3. **Beg, A. A., S. M. Ruben, R. I. Scheinman, S. Haskill, C. A. Rosen, and A. S. Baldwin, Jr.** 1992. I kappa B interacts with the nuclear localization sequences of the subunits of NF-kappa B: a mechanism for cytoplasmic retention. Genes Dev **6:**1899-913.
4. **Cortes, P., Z. S. Ye, and D. Baltimore.** 1994. RAG-1 interacts with the repeated amino acid motif of the human homologue of the yeast protein SRP1. Proc Natl Acad Sci U S A **91:**7633-7.
5. **Fagerlund, R., L. Kinnunen, M. Kohler, I. Julkunen, and K. Melen.** 2005. NF-{kappa}B is transported into the nucleus by importin {alpha}3 and importin {alpha}4. J Biol Chem **280:**15942-51.
6. **Ganchi, P. A., S. C. Sun, W. C. Greene, and D. W. Ballard.** 1992. I kappa B/MAD-3 masks the nuclear localization signal of NF-kappa B p65 and requires the transactivation domain to inhibit NF-kappa B p65 DNA binding. Mol Biol Cell **3:**1339-52.
7. **Gorlich, D., and U. Kutay.** 1999. Transport between the cell nucleus and the cytoplasm. Annu Rev Cell Dev Biol **15:**607-60.
8. **Hayden, M. S., and S. Ghosh.** 2004. Signaling to NF-kappaB. Genes Dev **18:**2195-224.
9. **Henkel, T., U. Zabel, K. van Zee, J. M. Muller, E. Fanning, and P. A. Baeuerle.** 1992. Intramolecular masking of the nuclear location signal and dimerization domain in the precursor for the p50 NF-kappa B subunit. Cell **68:**1121-33.
10. **Herbein, G., and W. A. O'Brien.** 2000. Tumor necrosis factor (TNF)-alpha and TNF receptors in viral pathogenesis. Proc Soc Exp Biol Med **223:**241-57.
11. **Kohler, M., S. Ansieau, S. Prehn, A. Leutz, H. Haller, and E. Hartmann.** 1997. Cloning of two novel human importin-alpha subunits and analysis of the expression pattern of the importin-alpha protein family. FEBS Lett **417:**104-8.
12. **Kohler, M., C. Speck, M. Christiansen, F. R. Bischoff, S. Prehn, H. Haller, D. Gorlich, and E. Hartmann.** 1999. Evidence for distinct substrate specificities of importin alpha family members in nuclear protein import. Mol Cell Biol **19:**7782-91.
13. **Krakauer, T., J. W. Leduc, and H. Krakauer.** 1995. Serum levels of tumor necrosis factor-alpha, interleukin-1, and interleukin-6 in hemorrhagic fever with renal syndrome. Viral Immunol **8:**75-9.
14. **Linderholm, M., C. Ahlm, B. Settergren, A. Waage, and A. Tarnvik.** 1996. Elevated plasma levels of tumor necrosis factor (TNF)-alpha, soluble TNF receptors, interleukin (IL)-6, and IL-10 in patients with hemorrhagic fever with renal syndrome. J Infect Dis **173:**38-43.
15. **Linderholm, M., P. H. Groeneveld, and A. Tarnvik.** 1996. Increased production of nitric oxide in patients with hemorrhagic fever with renal syndrome--relation to arterial hypotension and tumor necrosis factor. Infection **24:**337-40.
16. **Macara, I. G.** 1991. The ras superfamily of molecular switches. Cell Signal **3:**179-87.
17. **Nachury, M. V., U. W. Ryder, A. I. Lamond, and K. Weis.** 1998. Cloning and characterization of hSRP1 gamma, a tissue-specific nuclear transport factor. Proc Natl Acad Sci U S A **95:**582-7.
18. **Prescott, J., C. Ye, G. Sen, and B. Hjelle.** 2005. Induction of innate immune response genes by Sin Nombre hantavirus does not require viral replication. J Virol **79:**15007-15.
19. **Schmaljohn, C., and B. Hjelle.** 1997. Hantaviruses: a global disease problem. Emerg Infect Dis **3:**95-104.
20. **Schmaljohn, C. S., G. B. Jennings, J. Hay, and J. M. Dalrymple.** 1986. Coding strategy of the S genome segment of Hantaan virus. Virology **155:**633-43.
21. **Seki, T., S. Tada, T. Katada, and T. Enomoto.** 1997. Cloning of a cDNA encoding a novel importin-alpha homologue, Qip1: discrimination of Qip1 and Rch1 from hSrp1 by their ability to interact with DNA helicase Q1/RecQL. Biochem Biophys Res Commun **234:**48-53.
22. **Spiropoulou, C. F., C. G. Albarino, T. G. Ksiazek, and P. E. Rollin.** 2007. Andes and Prospect Hill hantaviruses differ in early induction of interferon although both can downregulate interferon signaling. J Virol **81:**2769-76.
23. **Thanos, D., and T. Maniatis.** 1995. NF-kappa B: a lesson in family values. Cell **80:**529-32.

24. **Verma, I. M., J. K. Stevenson, E. M. Schwarz, D. Van Antwerp, and S. Miyamoto.** 1995. Rel/NF-kappa B/I kappa B family: intimate tales of association and dissociation. Genes Dev **9:**2723-35.
25. **Wajant, H., K. Pfizenmaier, and P. Scheurich.** 2003. Tumor necrosis factor signaling. Cell Death Differ **10:**45-65.
26. **Wajant, H., and P. Scheurich.** 2004. Analogies between Drosophila and mammalian TRAF pathways. Prog Mol Subcell Biol **34:**47-72.
27. **Zabel, U., T. Henkel, M. S. Silva, and P. A. Baeuerle.** 1993. Nuclear uptake control of NF-kappa B by MAD-3, an I kappa B protein present in the nucleus. Embo J **12:**201-11.

APPENDICES:

FIGURE LEGENDS:

Fig. 1 The effect of HTNV N protein on NF-κB gene expression. (A) 293T cells were co-transfected with 500 ng of pNF-κB-hrGFP and 500 ng of either pWRG7077-Empty, pWRG7077-HTNV-S or pWRG7077-HTNV-M. After 24 h, cells were incubated in medium with or without TNF-α (0 to 100 ng/ml) for 4 h. As a positive control for inhibition in our assay, cells transfected with only 500 ng of pNF-κB-hrGFP were pretreated with 50 μM MG132 for 2 h before the addition of TNF-α and throughout the experiment. (B) Cells were co-transfected with 500 ng of pNF-κB-hrGFP and 5-500 ng of either pWRG7077-Empty, pWRG7077-HTNV-S or pWRG7077-HTNV-M. Or transfected with 500 ng of pNF-κB-hrGFP and treated with 0-50 μM MG132. After 24 h, cells were incubated in medium with or without TNF-α (10 ng/ml) for 4 h. After 4 h of treatment, medium was removed from all wells and replaced with medium lacking TNF-α for an additional 24 h. GFP expression was examined by fluorescence microscopy.

Fig. 2 Endogenous NF-κB transcription activation in cells expressing HTNV-S segment cDNA. A549 cells were transfected with 500 ng of pWRG7077-Empty, pWRG7077-HTNV-S, or pWRG7077-HTNV-M for 24 h. After treating the cells with 50 ng/ml of TNF-α for 15 min, cytoplasmic and nuclear extracts were prepared from lysates. (A) Nuclear extracts were allowed to bind to NF-κB consensus sequence oligos on 96-well plates followed by probing with antibodies specific for NF-κB p65 or NF-κB p50. Absorbance reading for each sample was determined using a spectrophotometer. (B) Cytoplasmic extracts were used for immunobloting to detect HTNV N protein and GAPDH. Statistical significance of the wild-type oligo+TNF was determined by comparing to the MUT oligo+TNF. Significance of N protein+TNF and MG132+TNF was determined by comparing to empty vector + TNF .

Fig. 3 Intracellular localization of NF-κB p65 in HTNV-S segment expressing cells. A549 cells were transfected with 500 ng of pWRG7077-Empty, pWRG7077-HTNV-S, pWRG7077-HTNV-M for 24 h. As a control for inhibition of nuclear translocation, some cells were pretreated with MG132 for 2 h before stimulation with TNF-α. After incubation, cells were left untreated or treated with 50 ng/ml of TNF-α for 15 min and fixed and stained with antibodies against NF-κB p65 (green), HTNV N or Gc? proteins (red) and stained with DAPI to highlight nuclei (blue).

Fig. 4 Examination of TNF-α-induced IκBα degradation and NF-κB p50 and p65 levels in HTNV-S segment expressing cells. A549 cells were transfected with 500 ng of pWRG7077-Empty, pWRG7077-HTNV-S, or pWRG7077-HTNV-M for 24 h. To induce degradation of IκBα, cells were treated with 50 ng/ml of TNF-α for 15 min and lysates were prepared for immunoblotting. For un-induced samples, cells were left untreated. Proteins were transferred to PVDF membranes and probed with antibodies against IκBα, p50, p65, HTNV N protein, or GAPDH.

Fig. 5 Analysis of HTNV-N protein interaction with importin α proteins. A549 cells were co-transfected with 0 μg or 1.25 μg of importin α1-FLAG, importin α2-FLAG, importin α3-FLAG, or importin α4-FLAG and 1.25 μg 7077-Empty or 7077-HTNV-S encoding plasmid. Immunoprecipitations (IP) were performed 24 h posttransfection with anti-HTNV-N protein antibody bound to sepharose beads. Immunoprecipitates and whole-cell lysates (WCL) were analyzed by western blotting (WB) for expression of importin α proteins and HTNV N protein.

Fig. 6 **Examination of TNF-α-induced NF-κB p65 nuclear translocation and degradation of IκBα in HTNV-infected cells.** A549 cells were mock-infected or infected with HTNV at an MOI of 5. On day 5, mock- and HTNV-infected cells were left untreated or treated with 50 ng/ml of TNF-α for 15 min. (A) After fixation, cells were stained with antibodies against NF-κB p65 (green), HTNV N protein (red), and stained with DAPI to

highlight nuclei (blue). Total cell lysates were prepared for immunoblotting and proteins were transferred to PVDF membranes. Blots were probed with antibodies against IκBα, p50, p65, HTNV N pro

Fig. 1

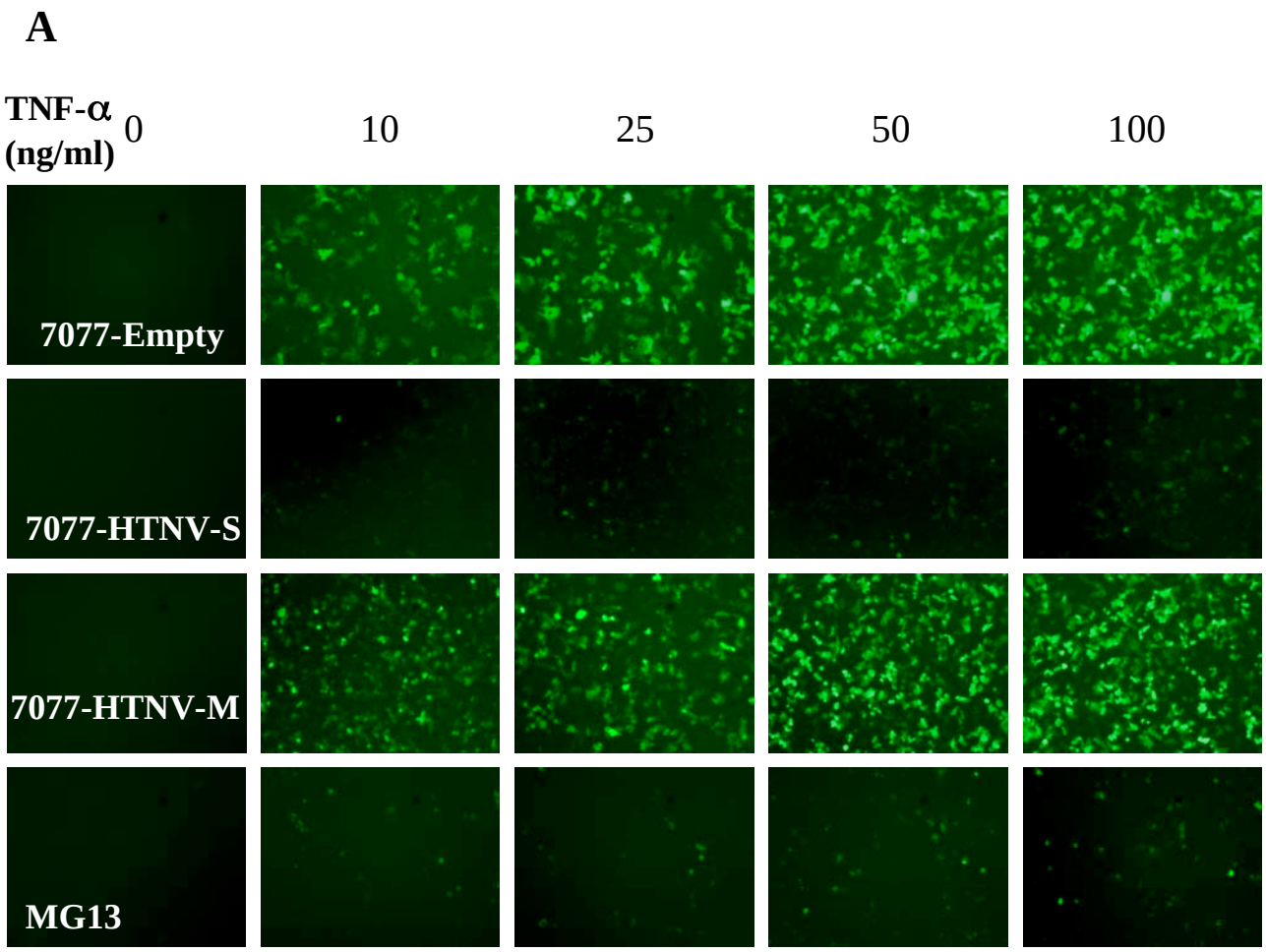
A
TNF-α (ng/ml)
0
10
25
50
100
7077-Empty
7077-HTNV-S
7077-HTNV-M
MG13

Fig. 1

B

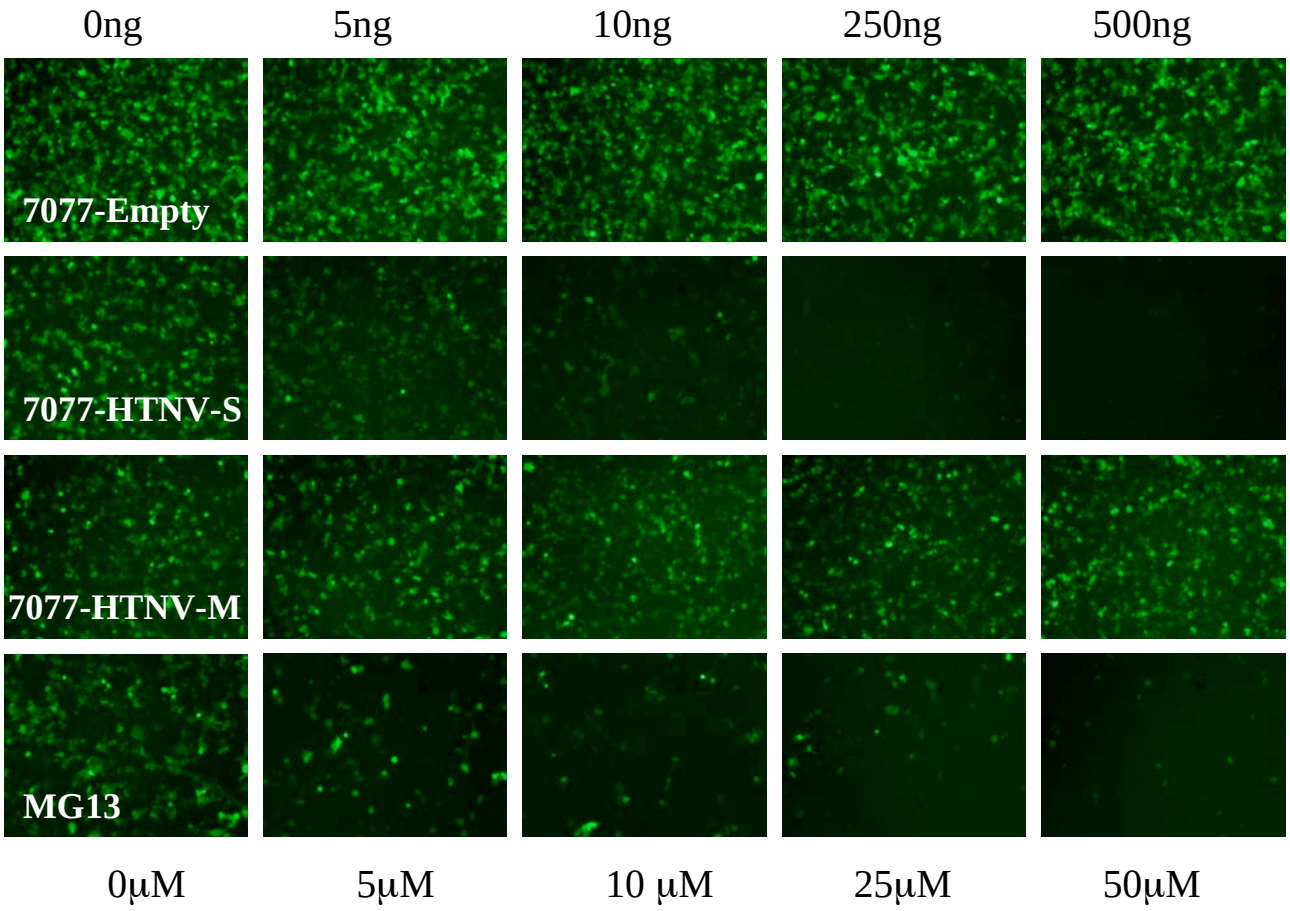
0ng
5ng
10ng
250ng
500ng
7077-Empty
7077-HTNV-S
7077-HTNV-M
MG13
0μM
5μM
10 μM
25μM
50μM

Fig. 2

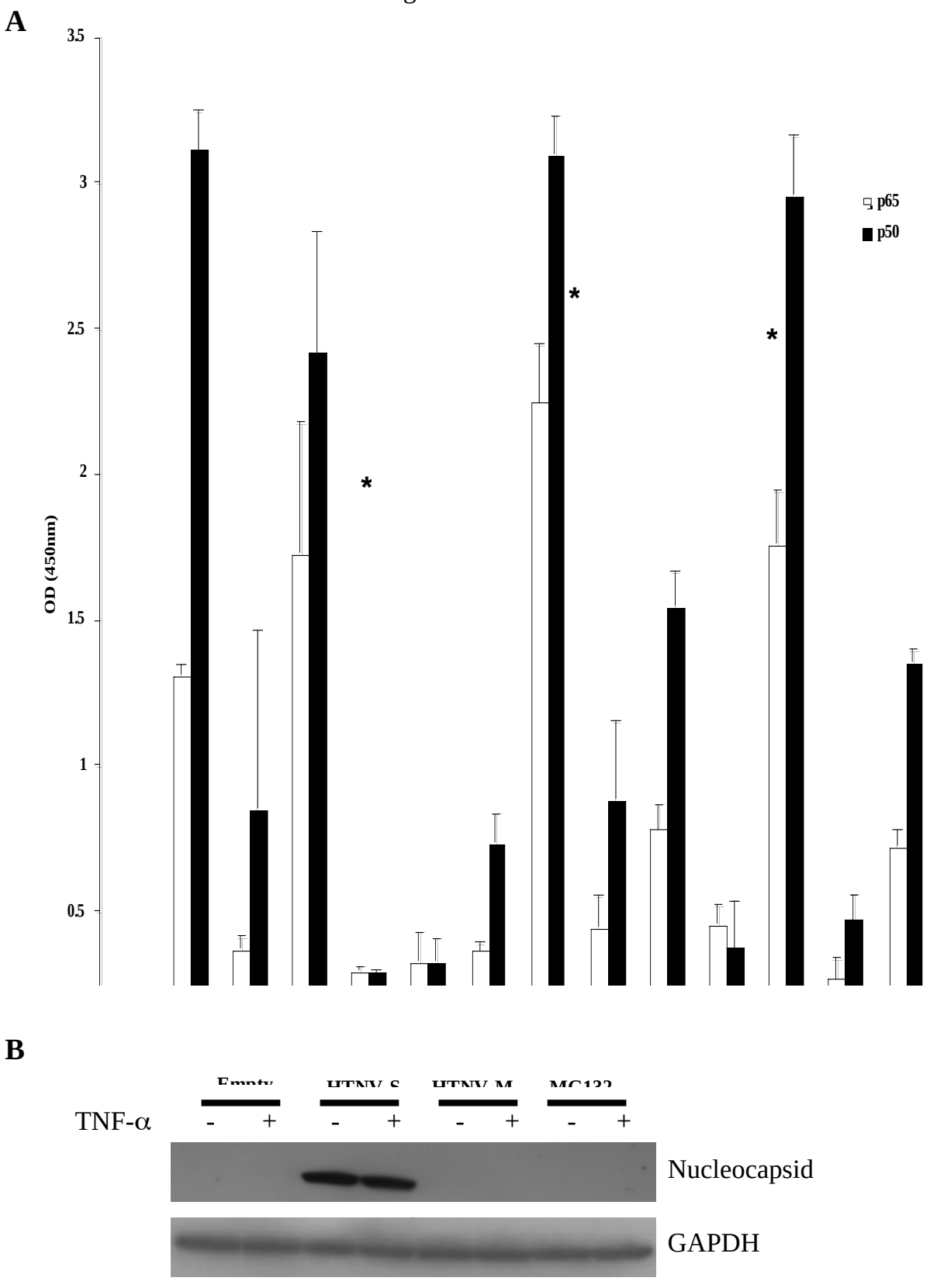
A
3.5
3
2.5
2
1.5
1
0.5
OD (450nm)
p65
p50
*
*
*
B
Empty
HTNV-S
HTNV-M
MG132
TNF-α
- + - + - + - +
Nucleocapsid
GAPDH

Fig. 3

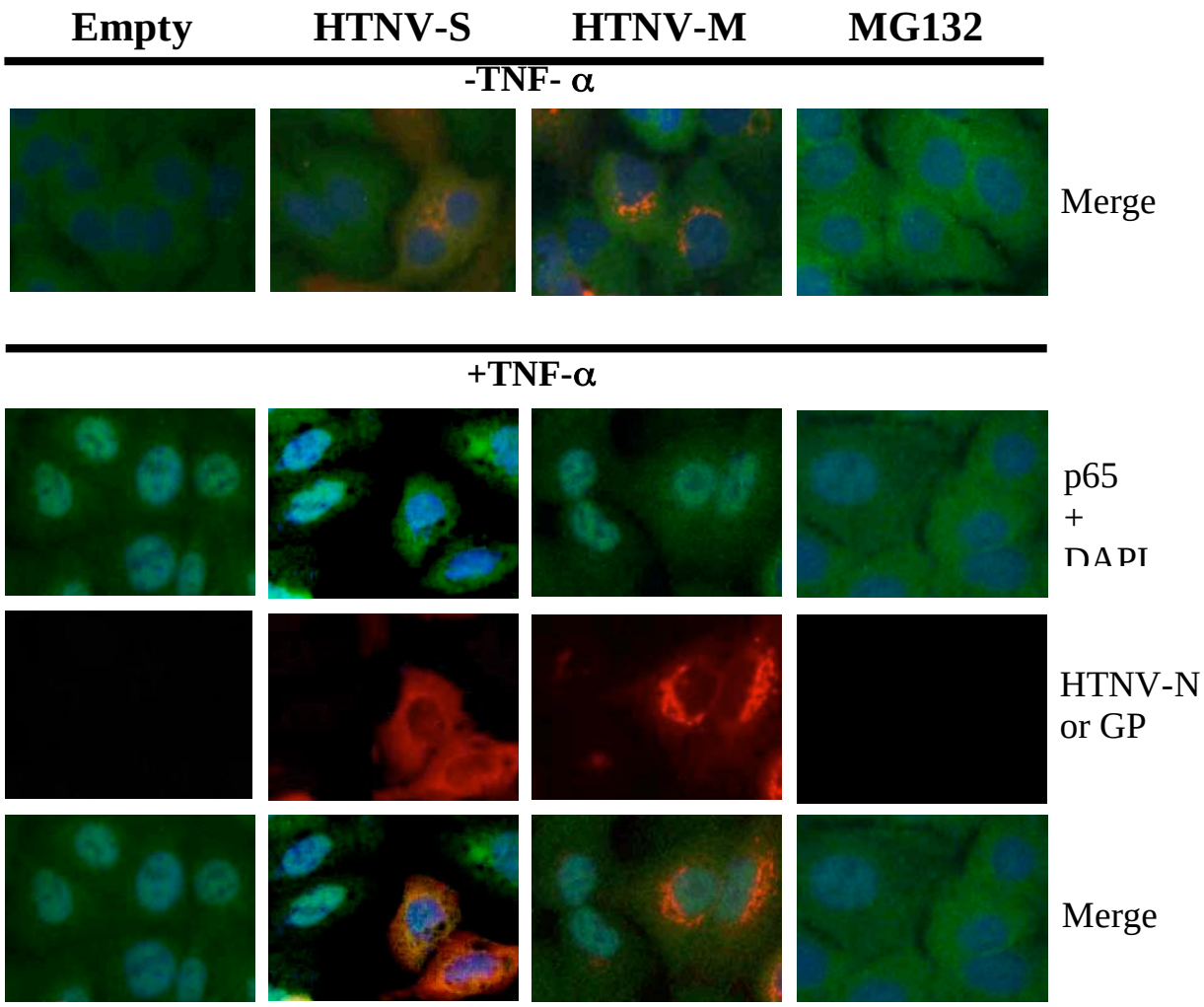
Empty
HTNV-S
HTNV-M
MG132
-TNF- α
Merge
+TNF-α
p65
+
DAPI
HTNV-N
or GP
Merge

Fig. 4

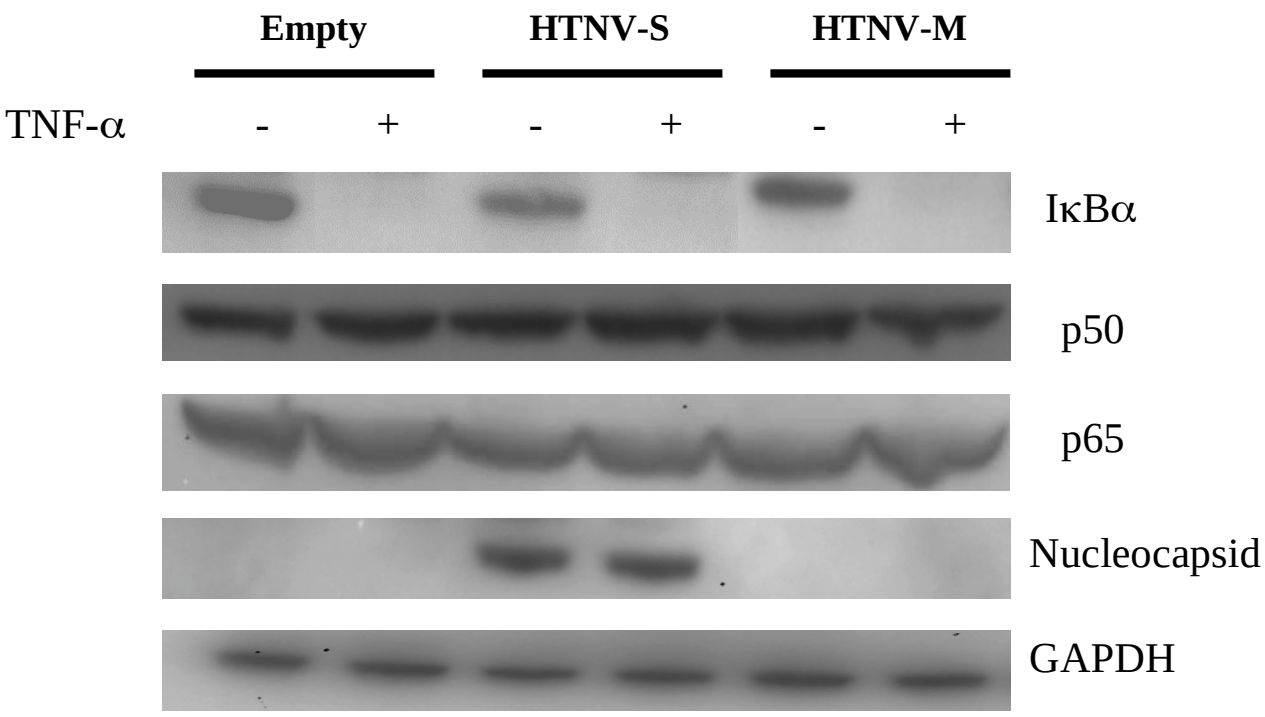

Fig. 5

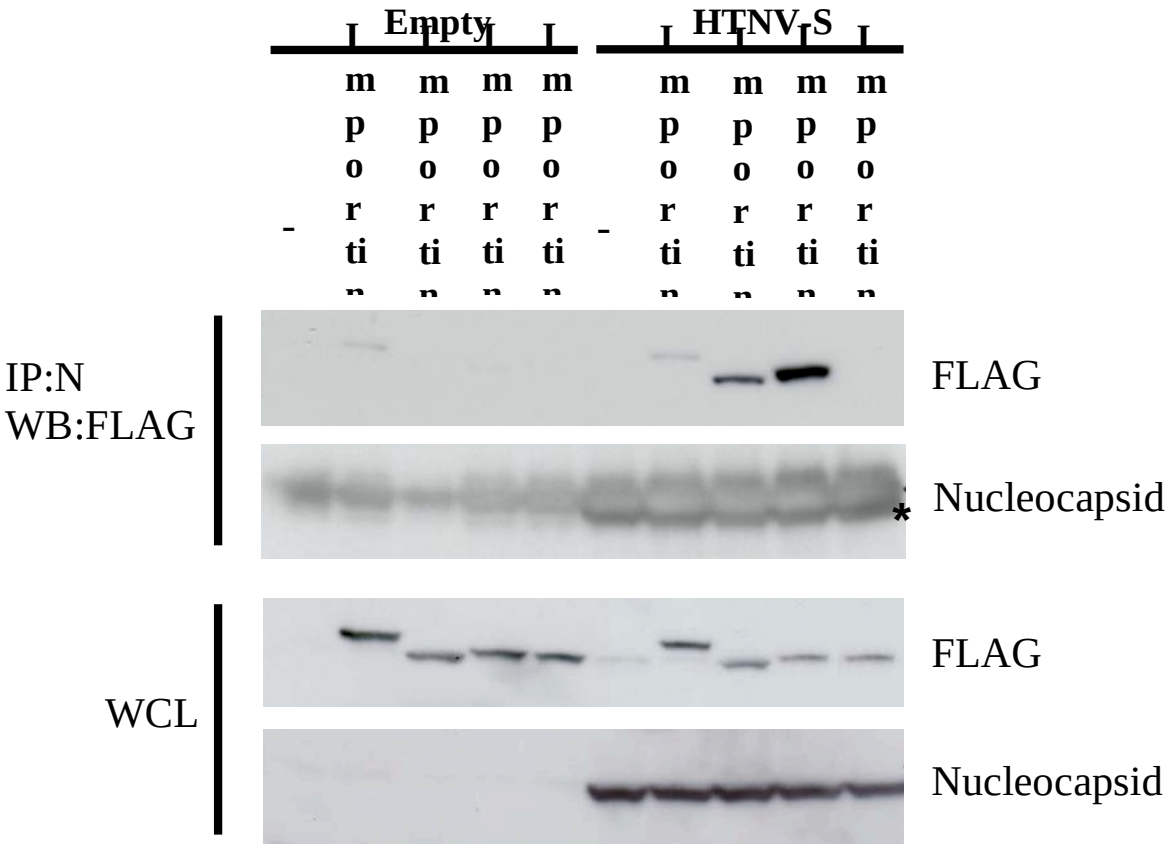
Empty
HTNV-S
-
mporin
-
mporin
IP:N
WB:FLAG
FLAG
Nucleocapsid
*
WCL
FLAG
Nucleocapsid

Fig. 6

A

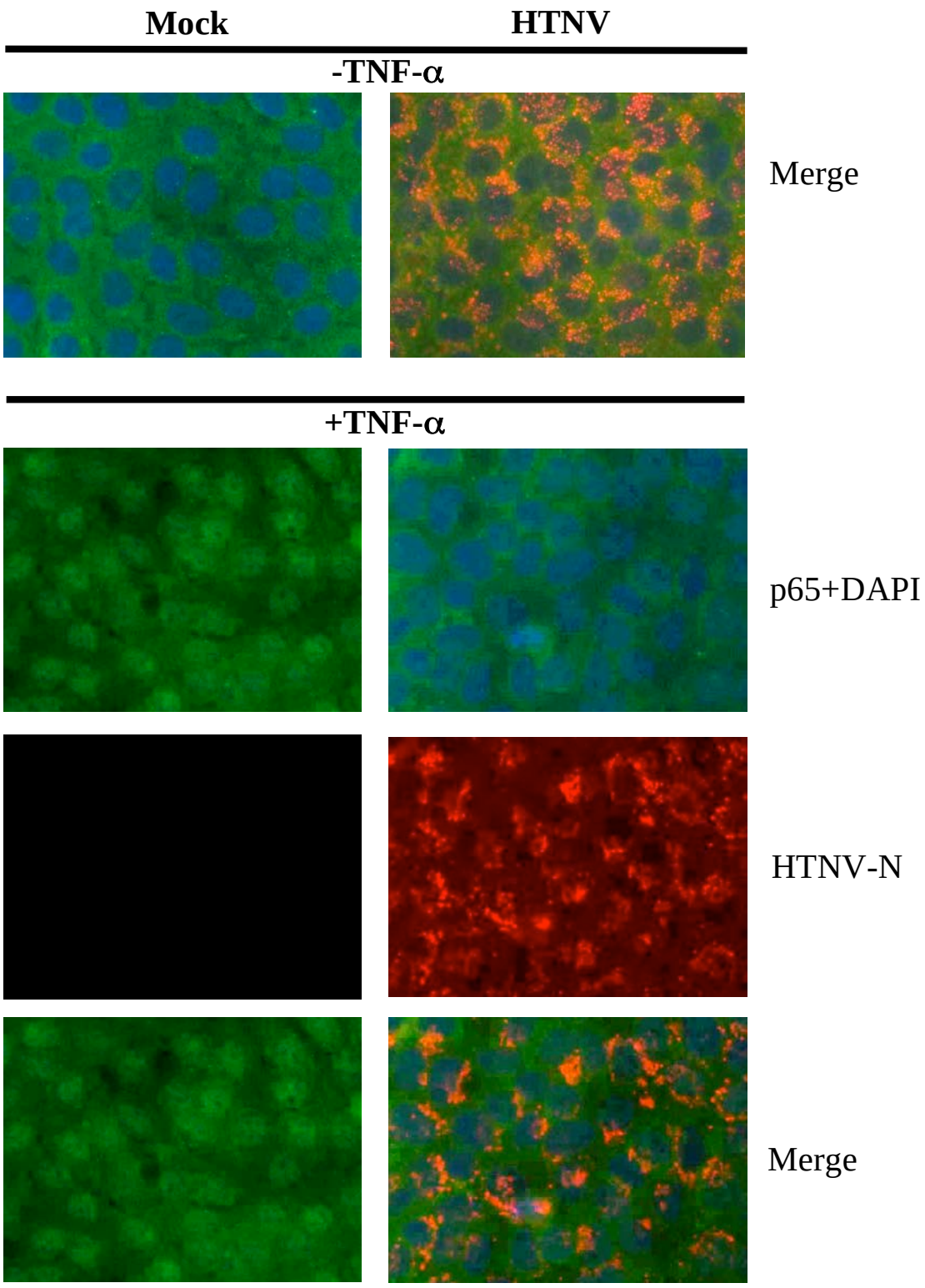

Fig. 6

B

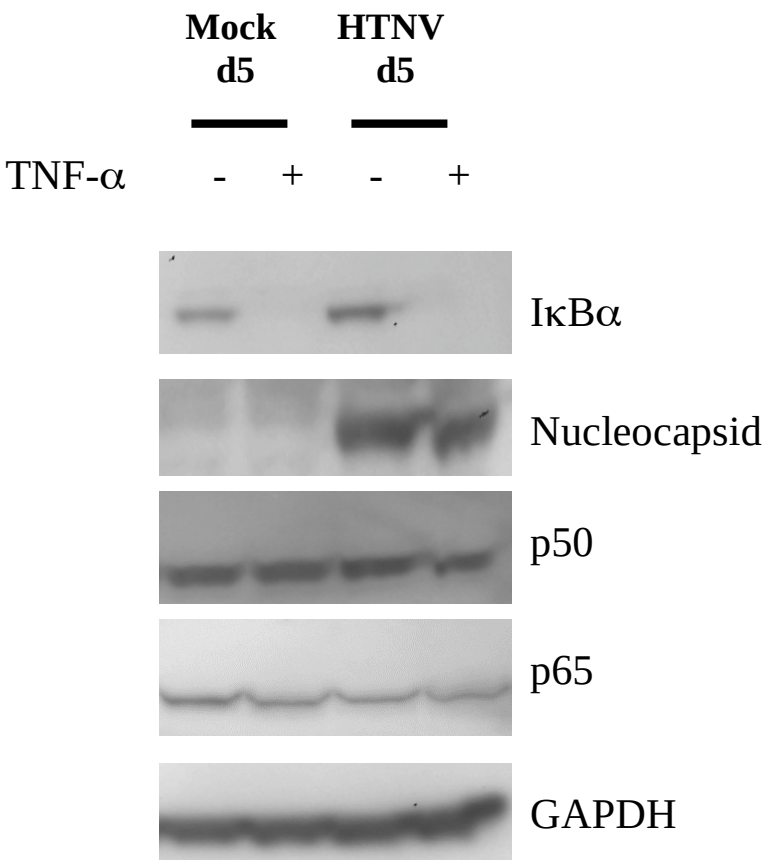

Cell Host & Microbe
Article

Ovarian Tumor Domain-Containing Viral Proteases Evade Ubiquitin- and ISG15-Dependent Innate Immune Responses

Natalia Frias-Staheli,[1,12] Nadia V. Giannakopoulos,[4,12] Marjolein Kikkert,[6] Shannon L. Taylor,[7] Anne Bridgen,[8] Jason Paragas,[9] Juergen A. Richt,[10] Raymond R. Rowland,[11] Connie S. Schmaljohn,[7] Deborah J. Lenschow,[4,5] Eric J. Snijder,[6] Adolfo García-Sastre,[1,2,3,*] and Herbert Whiting Virgin IV[4,*]
[1]Department of Microbiology
[2]Department of Medicine, Division of Infectious Diseases
[3]Emerging Pathogens Institute
Mount Sinai School of Medicine, New York, NY 10029, USA
[4]Department of Pathology and Immunology, Department of Molecular Microbiology
[5]Department of Medicine
Washington University School of Medicine, St. Louis, MO 63110, USA
[6]Molecular Virology Laboratory, Department of Medical Microbiology, Center of Infectious Diseases,
Leiden University Medical Center, LUMC, P.O. Box 9600, 2300 RC Leiden, The Netherlands
[7]United States Army Medical Research Institute for Infectious Diseases, Fort Detrick, MD 21702, USA
[8]Department of Biomedical Sciences, University of Ulster, Cromore Road, Coleraine BT52 1SA, UK
[9]Emerging Viral Pathogens Section, National Institute of Allergy and Infectious Diseases,
National Institutes of Health, Bethesda, MD 20892, USA
[10]National Animal Disease Center-ARS-USDA, Ames, IA 50010, USA
[11]Diagnostic Medicine and Pathobiology, Kansas State University, Manhattan, KS 66506, USA
[12]These authors contributed equally to this work.
*Correspondence: adolfo.garcia-sastre@mssm.edu (A.G.-S.), virgin@wustl.edu (H.W.V.)
DOI 10.1016/j.chom.2007.09.014

SUMMARY

Ubiquitin (Ub) and interferon-stimulated gene product 15 (ISG15) reversibly conjugate to proteins and mediate important innate antiviral responses. The ovarian tumor (OTU) domain represents a superfamily of predicted proteases found in eukaryotic, bacterial, and viral proteins, some of which have Ub-deconjugating activity. We show that the OTU domain-containing proteases from nairoviruses and arteriviruses, two unrelated groups of RNA viruses, hydrolyze Ub and ISG15 from cellular target proteins. This broad activity contrasts with the target specificity of known mammalian OTU domain-containing proteins. Expression of a viral OTU domain-containing protein antagonizes the antiviral effects of ISG15 and enhances susceptibility to Sindbis virus infection in vivo. We also show that viral OTU domain-containing proteases inhibit NF-κB-dependent signaling. Thus, the deconjugating activity of viral OTU proteases represents a unique viral strategy to inhibit Ub- and ISG15-dependent antiviral pathways.

INTRODUCTION

Viruses have evolved a panoply of different mechanisms to subvert cellular processes to their own advantage. In particular, viruses must overcome the potent antiviral and inflammatory effects of innate immune cytokines such as type I interferon (IFNαβ) and tumor necrosis factor alpha (TNFα). The induction and activity of these antiviral cytokines is controlled by, among other factors, Ub and Ub-like (UBL) molecules (Kirkin and Dikic, 2007). The activation of the transcriptional regulator nuclear factor-κB (NF-κB) by TNFα was one of the first immune regulatory pathways found to be dependent on protein ubiquitination (Karin and Ben-Neriah, 2000). NF-κB is sequestered in the cytoplasm of unstimulated cells through binding to IκB. TNFα binding to its receptor induces IκB phosphorylation followed by K^{48}-linked poly-ubiquitination targeting IκB for proteasomal degradation. This releases NF-κB dimers for translocation to the nucleus, where they regulate transcription. NF-κB-induced genes include type I IFN and other cytokines, hence this Ub-controlled pathway plays a vital role in innate and adaptive immunity, as well as in inflammation (Tergaonkar, 2006). In addition to ubiquitination of IκB, K^{63}- and K^{48}-linked ubiquitination regulates other molecules involved in this signaling pathway (Chen, 2005).

ISG15 is an interferon-induced UBL molecule with important antiviral activity against Sindbis, herpes simplex, influenza A, and influenza B viruses (Lenschow et al., 2007). ISG15, like Ub, is covalently conjugated to target proteins via a C-terminal LRLRGG sequence (Haas et al., 1987; Loeb and Haas, 1992; Narasimhan et al., 1996). Although conjugation is critical for the antiviral activity of ISG15 (Lenschow et al., 2005, 2007), the mechanism by which ISG15 mediates its antiviral function is not completely understood.

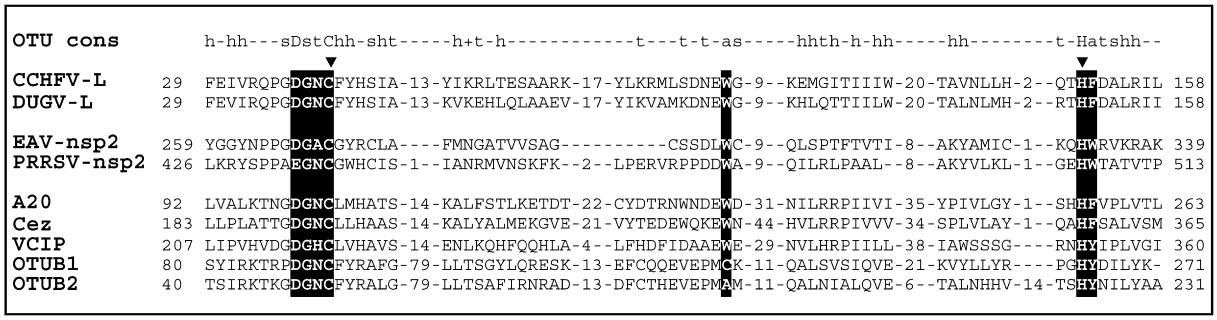

Figure 1. The OTU Domain Sequence Is Conserved across Viral and Mammalian Proteins

Multiple alignment of the OTU domains present in the proteins used in this study. In the consensus (Makarova et al., 2000), "h" indicates hydrophobic residues (A, C, F, L, I, M, V, W, Y, T, S, G), "s" indicates small residues (A, C, S, T, D, V, G, P), "+" indicates positively charged residues (R, K), "a" indicates aromatic residues (W, Y, F, H), and "t" indicates residues with high β-turn-forming propensity (A, C, S, T, D, E, N, V, G, P). Highly conserved residues are shaded in black. Numbers at the beginning and end of each sequence indicate the positions of the first and last aligned residue in the respective protein sequences; the numbers between aligned blocks indicate the numbers of residues that are not shown. CCHFV, Crimean Congo hemorrhagic fever virus; DUGV, Dugbe virus; EAV, equine arteritis virus; PRRSV, porcine respiratory and reproductive syndrome virus; VCIP, VCIP135; Cez, Cezanne; OTUB1 and OTUB2, Otubains 1 and 2, respectively.

Ub and ISG15 are synthesized as inactive precursors with C-terminal extensions that undergo cleavage to reveal the motif required for conjugation. Coordinated activities of an enzymatic cascade comprising an activating enzyme (E1), a conjugating enzyme (E2) and a ligase (E3) result in the conjugation of Ub or ISG15 to the ε-amino group of a lysine residue present in the target protein. Both Ub and ISG15 conjugation can be reversed by the activity of deconjugating enzymes. Deubiquitinating (DUB) proteolytic enzymes are also involved in processing of Ub precursors. Five classes of DUBs have been described (Nijman et al., 2005); one of the most recently identified is the ovarian tumor (OTU) domain family. This family comprises a group of putative cysteine proteases, homologous to the OTU protein in *Drosophila*, and includes more than a hundred proteins from eukaryotes, bacteria, and viruses (Makarova et al., 2000). Several OTU domain-containing mammalian proteins, such as Cezanne (Evans et al., 2003), Otubain 1 and 2 (Balakirev et al., 2003), and A20 (Evans et al., 2004) have been identified as proteases that participate in substrate-specific deubiquitinating processes. For example, A20 is an important downregulator of TNFα signaling via its deubiquitination of TRAF6 (Boone et al., 2004) and its dual function of poly-Ub^{63} deconjugation followed by poly-Ub^{48} modification of RIP (Wertz et al., 2004). These activities are mediated by its N-terminal OTU domain and its C-terminal zinc finger domain, respectively. However, the substrate specificity and physiologic role of most OTU domain-containing proteins remains unknown.

As protein ubiquitination and ISGylation are both important for innate immunity, rely on terminal LRLRGG sequences, and share a common mechanism of conjugation, we tested the hypothesis that viral OTU domain-containing proteases regulate Ub- and ISG15-dependent innate immunity via deconjugating protease activity. We found that two unrelated families of RNA viruses express OTU domain-containing proteases with the capacity to decrease Ub and ISG15 conjugation. Nairoviruses are negative-sense, segmented, RNA viruses of the *Bunyaviridae* family. Their large (L) protein contains an OTU domain and an RNA polymerase domain, placing this protein in the growing category of multifunctional viral proteins. Crimean Congo hemorrhagic fever virus (CCHFV) is a human nairovirus that causes hemorrhagic fever with up to 30% mortality (Whitehouse, 2004). Arteriviruses, including equine arteritis virus (EAV) and porcine respiratory and reproductive syndrome virus (PRRSV), are the causative agents of important diseases in horses and pigs. They are positive-sense, nonsegmented RNA viruses that contain an OTU domain within their nonstructural protein 2 (nsp2), which is also involved in viral replicase polyprotein processing (Snijder et al., 1995). We found that these viral OTU domains, in contrast to known mammalian OTU proteases, display a broad deconjugating activity toward ubiquitinated and ISGylated products and consequently inhibit innate immunity pathways that are dependent on Ub and ISG15. Thus, the deconjugating activity of viral OTU domains represents a unique strategy used by nairoviruses and arteriviruses to evade the host antiviral response, probably by targeting a common biochemical structure in Ub and the UBL protein ISG15.

RESULTS

OTU Domains in Viral and Mammalian Proteins

Sequencing of the L gene of the highly pathogenic human virus CCHFV (NFS and AGS, data not shown) (Honig et al., 2004; Kinsella et al., 2004) led to the identification of an OTU domain in the N-terminal region of the viral protein (Figure 1). This domain was also present in the L proteins of the nairoviruses Dugbe virus (DUGV) and Nairobi sheep disease virus (Honig et al., 2004) but has not been found in the L proteins of any other genus in the *Bunyaviridae*

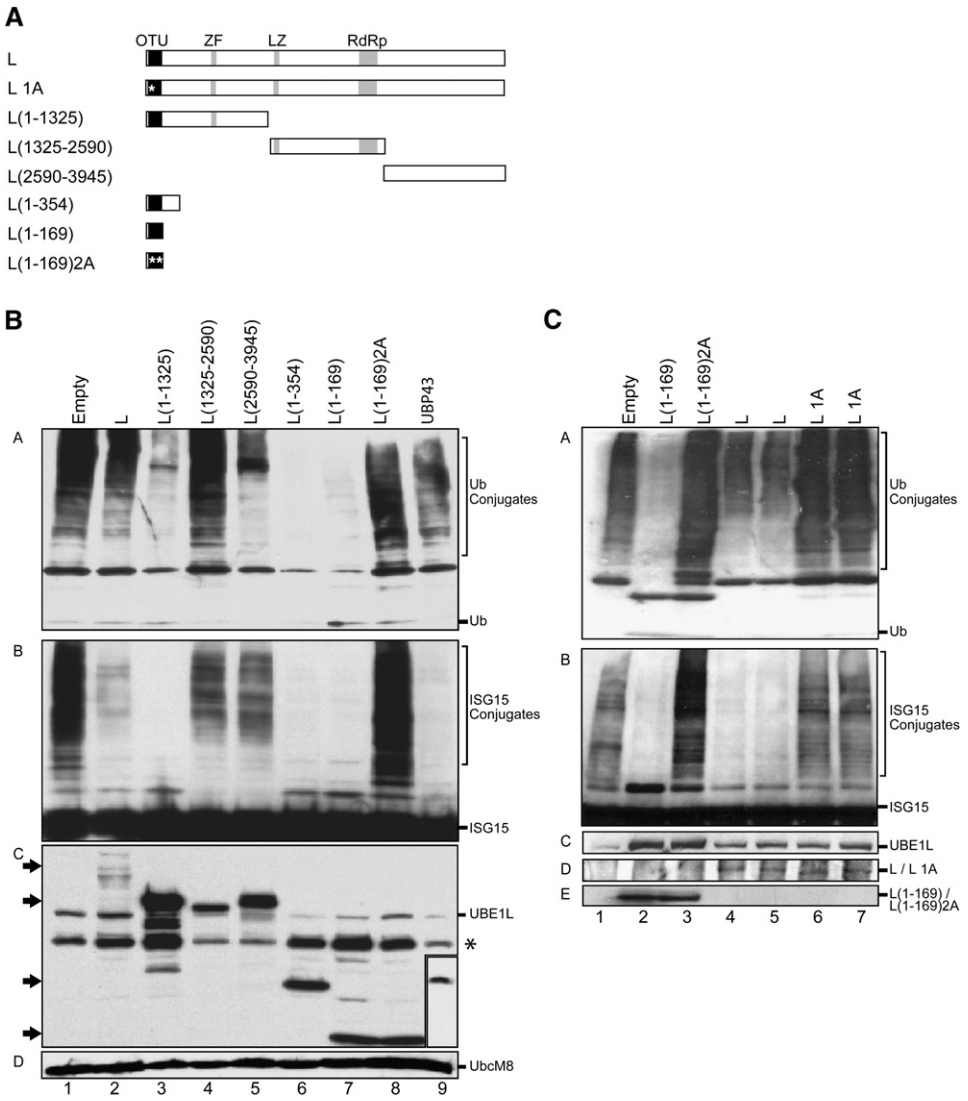

Figure 2. Levels of Ubiquitinated and ISGylated Proteins in Cells Expressing CCHFV-L and CCHFV-L Mutants

(A) Schematic representation of the CCHFV-L constructs utilized in these studies. Predicted protein domains within the protein: OTU domain; ZF, zinc finger; LZ, leucine zipper; RdRp, RNA-dependent RNA polymerase conserved motifs. White stars represent mutations in the OTU domain: 1A (C40A) or 2A (C40A and H151A). All constructs were HA tagged.

(B) 293T cells were transfected with either HA-Ub (panel A) or His-ISG15, HA-mUBE1L, and Flag-UbcM8 (panels B–D) along with HA-tagged CCHFV-L constructs, Flag-UBP43, or empty plasmid. Total protein ubiquitination was visualized by immunoblotting with anti-HA (panel A), and protein ISGylation was visualized by anti-ISG15 immunoblot (panel B). ISG15-transfected samples were also probed with anti-HA or anti-Flag (panels C and D) for detection of the CCHFV-L constructs (left arrows), mUbE1L, UBP43 (inset), and UbcM8. Asterisk indicates a nonspecific band.

(C) L and L 1A were analyzed for their effect on total ubiquitination (panel A) or ISGylation (panel B) as described in (B). Expression of HA-tagged UBE1L (panel C), L and L 1A (panel D), and L(1–169) and L(1–169)2A (panel E) is shown.

family. An alignment of the OTU domains present in nairoviruses, arteriviruses, and mammalian proteins A20, Cezanne, VCIP135, Otubain 1, and Otubain 2 revealed limited identity; however, a strong conservation of D^{37}, G^{38}, N^{39}, C^{40}, W^{71}, H^{151}, and an aromatic amino acid at position 152 (numbering based on the CCHFV-L sequence) was observed (Figure 1, black boxes). Among these amino acids, C^{40} and H^{151} (Figure 1, black arrows) were predicted to be the catalytic residues present in the putative protease active site (Balakirev et al., 2003; Makarova et al., 2000; Nanao et al., 2004; Snijder et al., 1995).

Impact of CCHFV-L Expression on Protein Ubiquitination and ISGylation

Given that host OTU domain proteins have deubiquitinating activity (Nijman et al., 2005), we tested the hypothesis that the L protein of CCHFV (CCHFV-L) has deubiquitinating and deISGylating activity (Figure 2). Transfection of

cells with plasmids expressing CCHFV-L slightly decreased the overall expression of Ub-conjugated proteins (Figure 2B, lanes 1 and 2, panel A; Figure 2C, lanes 1, 4, and 5, panel A). To test the effect of CCHFV-L expression on protein ISGylation, ISG15 conjugates were generated by transfecting plasmids expressing ISG15 and its specific E1 (UBE1L) (Yuan and Krug, 2001) and E2 (UbcM8) (Kim et al., 2004; Zhao et al., 2004) enzymes, since endogenous levels of ISGylated proteins are low in the absence of IFN stimulation. Cotransfection of CCHFV-L resulted in a clear decrease in the level of ISGylated proteins (Figure 2B, lanes 1 and 2, panel B; Figure 2C, lanes 1, 4, and 5, panel B). This decrease was also observed when CCHFV-L was untagged (data not shown). The decrease in total ISGylation was comparable to the effect of UBP43, a known ISG15 deconjugating enzyme (Figure 2B, lane 9, panel B). Expression of CCHFV-L did not affect levels of expression of UBE1L or UbcM8 (Figure 2B, lane 2, panels C and D; Figure 2C, lanes 4 and 5, panel C), consistent with CCHFV-L acting via inhibition of ubiquitination and ISGylation reactions or by directly deubiquitinating or deISGylating proteins.

The OTU Domain of CCHFV-L Decreases the Levels of Ubiquitinated and ISGylated Proteins

To determine the region of the L protein responsible for decreasing ubiquitinated and ISGylated proteins, plasmids expressing three portions of the L protein were constructed (Figure 2A). Expression of the OTU domain-containing N-terminal portion, L(1–1325), resulted in the greatest decrease of Ub and ISG15 conjugates (Figure 2B, lane 3, panels A and B). To further map this region, truncation mutants of the L protein expressing only the first 354, L(1–354), or 169 amino acids, L(1–169), were tested. The results indicated that the region responsible for the decreased levels of Ub and ISG15 conjugates mapped to the OTU domain, L-(1–169) (Figure 2B, lanes 6 and 7, panels A and B; Figure 2C, lane 2, panels A and B).

The Predicted Protease Active Site of the CCHFV-L OTU Domain Is Required for Reducing Ub and ISG15 Conjugates

To test whether the amino acids C^{40} and H^{151} (Figure 1, black arrows) were critical for the observed reduction in ubiquitinated and ISGylated proteins by the CCHFV-L OTU domain, we expressed a full-length L protein with a C^{40} to A^{40} mutation (L 1A) and a mutant L(1–169) protein in which both amino acids were replaced by alanines [L(1–169)2A] (Figure 2A). Expression of L 1A and L(1–169)2A proteins did not decrease levels of ubiquitinated or ISGylated proteins (Figure 2B, lane 8, panels A and B; Figure 2C, lanes 3, 6, and 7, panels A and B), strongly suggesting that the OTU domain contains a cysteine protease activity that mediates the decrease in ubiquitinated and ISGylated proteins.

The OTU Domain of CCHFV-L Is a Deconjugating Enzyme with Specificity for Poly-Ub Conjugates and ISG15

To determine whether the CCHFV-L OTU domain directly deconjugates Ub and ISG15 from target proteins, we expressed and purified L(1–169) and a catalytic C^{40} to A^{40} mutant, L(1–169)1A, for in vitro deconjugation assays (Figure 3A). Recombinant L(1–169) cleaved both K^{48}- and K^{63}-linked poly-Ub chains into monomers (Figure 3B, lanes 2 to 5), similarly to isopeptidase T, a known DUB enzyme (Figure 3B, lane 10). This activity was markedly decreased by mutating the amino acid C^{40} (Figure 3B, lanes 6 to 9), indicating that this residue is required for optimal protease activity. The small amount of deconjugation observed with L(1–169)1A is not unexpected, as mutation of Cezanne's catalytic cysteine yielded similar data where most, but not all, catalytic activity was impaired (Evans et al., 2003). This result shows that the OTU domain of CCHFV-L has bona fide DUB activity in the absence of other cellular proteins.

We next determined whether L(1–169) can deconjugate ISGylated proteins. For this, we generated cell lysates from IFNβ-treated *Ubp43*$^{-/-}$ murine embryonic fibroblasts (MEFs) that are rich in ISG15 conjugates (Malakhov et al., 2003). Incubation of these lysates with recombinant L(1–169) protein, but not L(1–169)1A, appreciably decreased ISGylated proteins (Figure 3C, top panel) in a L(1–169) concentration-dependent manner. This result suggests that the CCHFV OTU domain has C^{40}-dependent ISG15 deconjugating activity but does not exclude the possibility that the protease activity of the viral OTU domain was activating another deISGylating enzyme present in cell lysates. To address this possibility, we enriched 6xHisISG15 conjugates using affinity chromatography. Incubation of ISG15 conjugates with increasing amounts of L(1–169) resulted in ISG15 deconjugation (Figure 3C, lanes 2 to 5, bottom panel). No deconjugation was detected with the mutant L(1–169)1A protein (Figure 3C, lanes 6 to 9, bottom panel). In addition, L(1–169) processed a pro-ISG15 protein into its mature form (Figure 3E, lane 2, panel A). These data suggest that the CCHFV-L OTU domain directly deconjugates ISGylated proteins through its predicted cysteine protease activity.

To gain further insights on the specificity of the OTU domain, we assessed the ability of L(1–169) and L(1–169)1A to hydrolyze poly-SUMO-2 (Figure 3D, top panel) and poly-SUMO-3 chains (Figure 3D, bottom panel), pro-SUMO-1 (Figure 3E, panel C), and pro-Nedd8 (Figure 3E, panel B). While the catalytic domain of SENP2 ($SENP2_{CD}$), a SUMO-specific protease, could hydrolyze SUMO chains to monomers (Figure 3D, lane 10) and process pro-SUMO-1 (Figure 3E, lane 5, panel C), neither L(1–169) nor L(1–169)1A was able to cleave SUMO chains or a pro-SUMO-1 precursor. However, similar to its ability to process pro-ISG15 (Figure 3E, lane 2, panel A), L(1–169) hydrolyzed pro-Nedd8 into a mature form (Figure 3E, lane 2, panel B). In summary, the OTU domain of CCHFV-L hydrolyzes Ub and ISG15, but not SUMO-2 or SUMO-3,

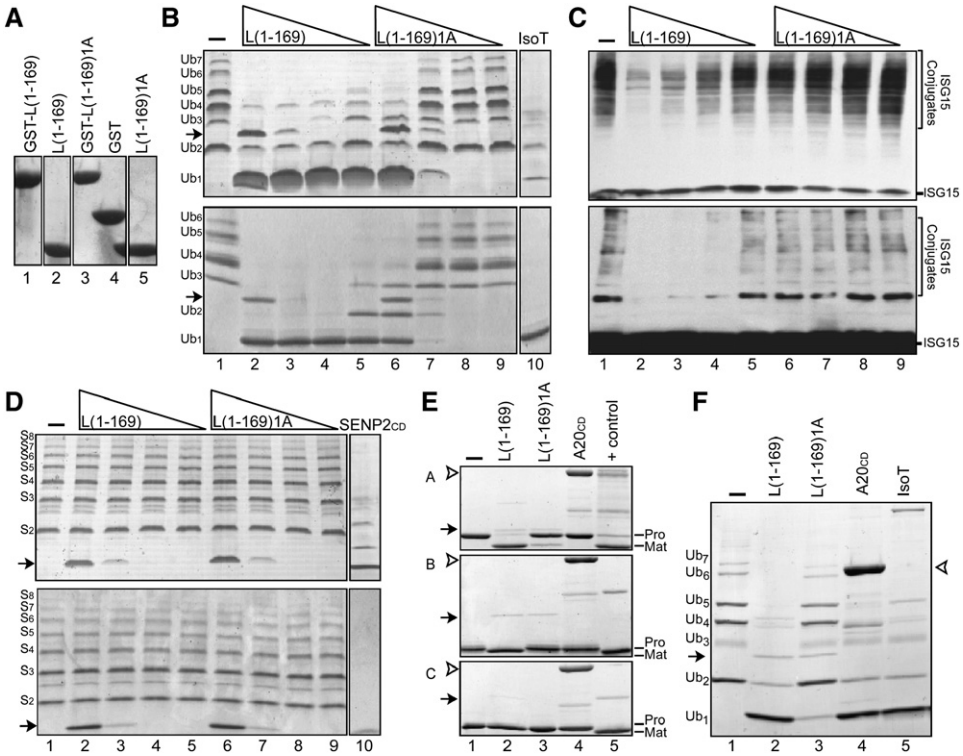

Figure 3. In Vitro Ub and ISG15 Deconjugation Activities of the CCHFV-L OTU Domain

(A) Coomassie-stained gel of GST-L(1–169), L(1–169), GST-L(1–169)1A, and L(1–169)1A recombinant proteins. L(1–169) and L(1–169)1A proteins were used for the in vitro experiments.

(B) K^{48} (top panel)- or K^{63} (bottom panel)-linked poly-Ub chains were incubated with reaction buffer (lane 1) or 10-fold dilutions of L(1–169) or L(1–169)1A recombinant proteins, subjected to SDS-PAGE and visualized by Coomassie staining. Isopeptidase T (IsoT) was used as a positive control. Black arrows indicate L(1–169) and L(1–169)1A proteins.

(C) Lysates of *Ubp43*$^{-/-}$ MEFs (top panel) or ISG15 conjugates purified from ISG15, HA-mUBE1L, and Flag-UbcM8 transfected 293T cells (bottom panel) were incubated with reaction buffer (lane 1) or 10-fold dilutions of L(1–169) or L(1–169)1A protein. ISG15 conjugates were visualized by anti-ISG15 immunoblot.

(D) SUMO-2 (top panel) or SUMO-3 (bottom panel) chains were incubated with reaction buffer (lane 1) or 10-fold dilutions of L(1–169) or L(1–169)1A and visualized by Coomassie staining. His_6-$SENP2_{CD}$ was used as a positive control. Black arrows indicate L(1–169) and L(1–169)1A proteins. S_{2-8} indicates number of SUMO-2 or SUMO-3 molecules.

(E and F) ProISG15 (panel A), proNedd8 (panel B), proSUMO-1 (panel C) or K^{48}-linked Ub (F) chains were incubated with reaction buffer, L(1–169), L(1–169)1A, or A20 catalytic domain ($A20_{CD}$) and visualized by Coomassie staining. Positive controls indicate incubation with UBP43 (panel A), NEDP1 (panel B), $SENP2_{CD}$ (panel C), or IsoT (F). Black arrows indicate L(1–169) and L(1–169)1A proteins, and white arrowhead indicates $A20_{CD}$. "Pro" indicates the pro-UBL molecule form, and "Mat" indicates the mature protein.

from conjugates in vitro, suggesting that viral OTU domains have the unique ability to recognize Ub and specific UBL molecules.

Additional Viral OTU Domains Mediate Deubiquitination and DeISGylation

In addition to CCHFV, viral OTU domains are found in the L proteins of other nairoviruses and in the nsp2 proteins of arteriviruses such as EAV and PRRSV (Figure 1). The arterivirus nsp2 cysteine protease cleaves the nsp2/nsp3 site within the large viral polyprotein during replicase maturation. In the case of EAV, this process is known to be mediated by the 166 N-terminal residues of nsp2, which contains the OTU domain (Snijder et al., 1995). In our study, a slightly larger N-terminal EAV-nsp2 domain (175 amino acids; nsp2N) was used in addition to the full-length protein. The OTU domain of the L protein of DUGV, a nairovirus related to CCHFV, as well as EAV-nsp2, EAV-nsp2N, and PRRSV-nsp2, decreased Ub and ISG15 conjugates when expressed in 293T cells (Figure 4A, lanes 3–6), indicating that deconjugation may be an immune evasion strategy shared by diverse viral families.

Previous studies have demonstrated that the OTU domain-containing mammalian proteins Otubain 1, Otubain 2, Cezanne, VCIP135, and A20 cleave poly-Ub chains in vitro (Balakirev et al., 2003; Evans et al., 2003, 2004; Wang et al., 2004). In contrast, only overexpression of Otubain 1 and Cezanne moderately decreased cellular global Ub conjugate levels, while expression of A20 or Otubain 2 had no effect on total levels of ubiquitinated proteins (Balakirev et al., 2003; Evans et al., 2003, 2004). To date, there have been no published studies investigating the effects of these proteins on ISG15 conjugates. We therefore tested Otubain 1, Otubain 2, Cezanne, VCIP135, and A20 for their

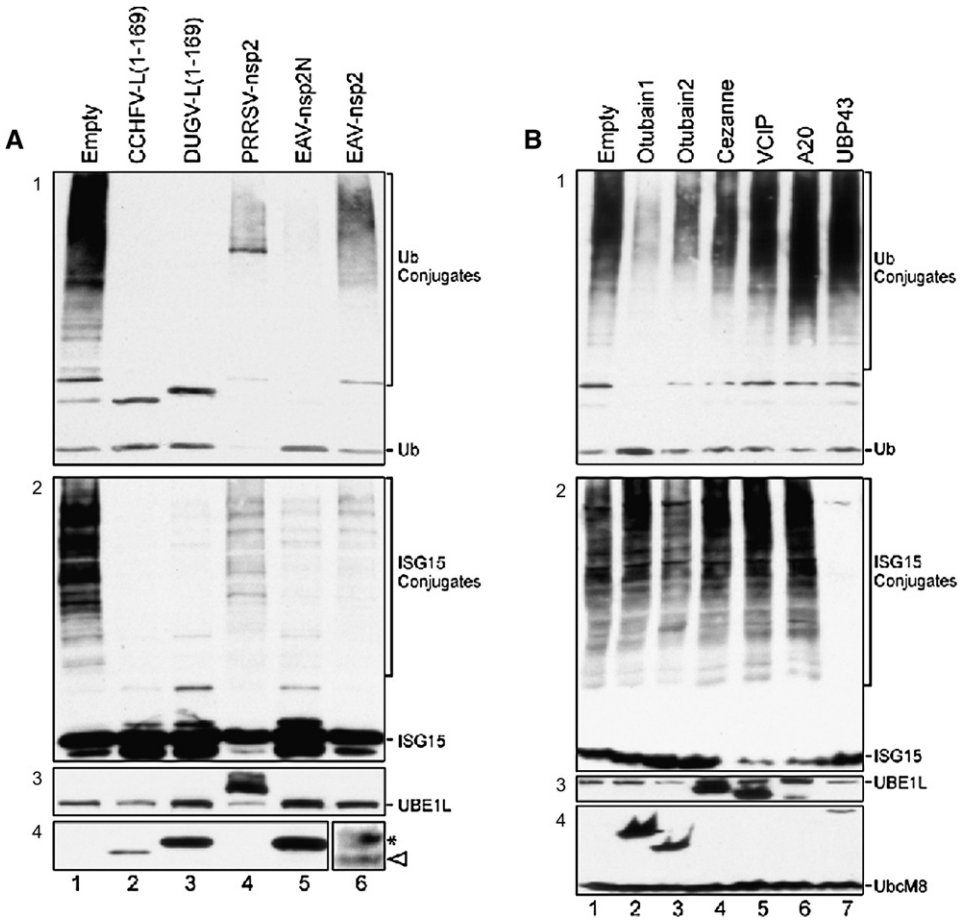

Figure 4. Ub and ISG15 Deconjugation Activity of OTU Domain-Containing Polypeptides of Viral and Mammalian Origin

(A) CCHFV-L(1–169), DUGV-L(1–169), PPRSV-nsp2, EAV-nsp2N, or EAV-nsp2 were cotransfected into 293T cells with either HA-Ub (panel 1) or ISG15, HA-mUBE1L, Flag-UbcM8, and Herc5 plasmids (panels 2 and 3). Samples were immunoblotted for HA (panel 1) or ISG15 (panel 2). ISG15-transfected samples were also probed with anti-HA (panel 3) or anti-Flag plus anti-HA (panel 4) to show expression of HA-mUBE1L, PPRSV-nsp2, CCHFV-L(1–169), DUGV-L(1–169), EAV-nsp2N, or EAV-nsp2 (inset, open triangle). Asterisk indicates a nonspecific band.

(B) Otubain 1, Otubain 2, Cezanne, VCIP135, A20, or UBP43 were analyzed for their effect on total ubiquitination (panel 1) or ISGylation (panels 2–4) as described in (A). Expression of HA-tagged Cezanne and VCIP135 (panel 3) and Flag-tagged Otubain 1 and 2 and UBP43 (panel 4) is shown.

ability to decrease overall protein ubiquitination and ISGylation in transfected cells (Figure 4B). Expression of Otubain 1 resulted in a significant decrease in Ub conjugate levels, while Otubain 2 and Cezanne had a lesser effect (Figure 4B, lanes 2–4, panel 1). Consistent with their specificity for particular ubiquitinated substrates, expression of VCIP135 and A20 did not result in a decrease in overall ubiquitination. None of the OTU-containing mammalian proteins tested decreased global levels of ISG15 conjugates (Figure 4B, lanes 2–6, panel 2). Similar results were obtained when truncation mutants expressing the OTU domains of Otubain 1, Otubain 2, Cezanne, and A20 were tested (data not shown). In addition, the OTU-containing catalytic domain of A20 ($A20_{CD}$) was unable to process either ISG15 or Nedd8 (Figure 3E, lane 4, panels A and B), even though it cleaved K^{48}-linked Ub chains (Figure 3F, lane 4). By contrast, overexpression of the mammalian deISGylating enzyme UBP43 decreased overall levels of ISG15 conjugates but not Ub conjugates (Figure 4B, lane 7). Thus, viral OTU proteases appear to be unique in their ability to target both ISG15 and Ub conjugates.

Transgenic Mice Expressing CCHFV-L(1–1325) Have Increased Susceptibility to Sindbis Virus Infection

To assess the effect of expressing an OTU domain during viral infection, we generated transgenic mice expressing the CCHFV-L(1–1325) OTU domain-containing protein, which exhibits DUB and deISGylating activities (Figure 2B, lane 3). We obtained germline transgene transmission in three lines designated 1836, 1854, and 2929, and we evaluated L(1–1325) expression in both MEFs and brain lysates from these transgenic lines. MEF cells and brain tissue from 1836 transgenic mice contained detectable L(1–1325) protein, while protein expression from the 1854 and 2929 lines was either undetectable or very low (Figures 5A and 5B). We next evaluated the

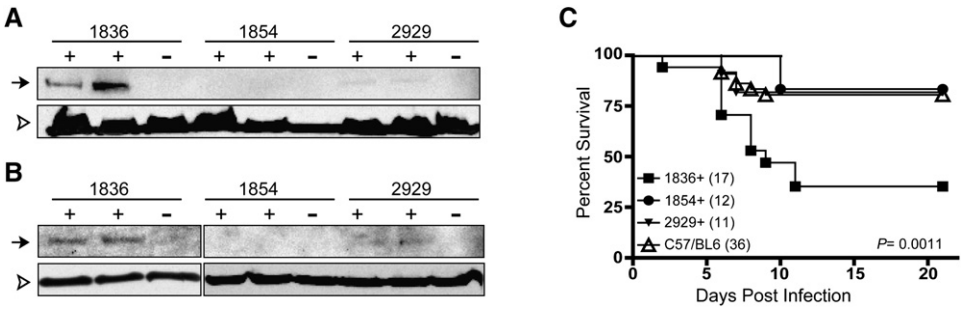

Figure 5. Expression of L(1–1325) Transgene Correlates with Increased Susceptibility to Sindbis Virus Infection

(A and B) Expression of L(1–1325) transgene and actin in MEFs (A) and brain lysates (B). + indicates a transgene-positive mouse, and − indicates a C57/BL6 mouse. The arrows indicate L(1–1325) protein and open triangles denote actin.

(C) Survival of L(1–1325) transgenic mice following infection with Sindbis virus AR86. Transgene-negative littermates from 1836, 1854, and 2929 served as C57/BL6 controls. Numbers of mice in each group are indicated in parenthesis. Comparison by statistical analysis was made between 1836+ and C57/BL6 ($p = 0.0011$).

sensitivity of L(1–1325) transgenic mice to infection with the virulent Sindbis virus strain AR86, an alphavirus that causes lethal encephalitis in young mice and is sensitive to ISG15-mediated antiviral effects (Lenschow et al., 2005). Susceptibility to Sindbis virus infection tracked with expression of the L(1–1325) protein (Figure 5C). Thirty-five percent of mice from the 1836 transgenic line survived infection compared to ≥80% survival in C57/BL6 littermate controls or transgenic mice expressing low or undetectable levels of transgene-encoded protein. The decreased survival of line 1836 transgenic mice following AR86 infection suggests that CCHFV-L OTU enhances susceptibility to viral disease in vivo.

The OTU Domain of CCHFV Overcomes ISG15-Mediated Protection from Sindbis Virus-Induced Lethality

The increased pathogenicity of Sindbis virus observed in L(1–1325)-expressing mice suggested that the CCHFV-L OTU domain might counteract the antiviral activities of ISG15 in vivo. It was previously shown that expression of ISG15 from the chimeric Sindbis virus dsTE12Q protects adult *IFNαβR*$^{-/-}$ mice from Sindbis virus-induced lethality (Lenschow et al., 2005). To determine whether expression of the CCHFV-L OTU domain would antagonize this protective effect of ISG15, we engineered four recombinant chimeric Sindbis viruses (Figure 6A). Two viruses expressed ISG15 followed by an IRES element to drive translation of either L(1–169) (169GG) or enzymatically inactive L(1–169)2A (MTGG). We also generated control viruses that expressed either L(1–169) (169) or L(1–169)2A (MT) in the absence of ISG15.

The recombinant viruses expressed the OTU domains and ISG15 as expected (Figures S1A and S1B in the Supplemental Data available with this article online) as well as similar levels of Sindbis virus proteins in infected cells (Figure S1C). All four viruses grew with similar kinetics to similar final titers under single-step growth conditions in BHK-21 cells (Figure S2). This is expected, as to date ISG15 has only demonstrated antiviral activity in vivo.

We assessed the ability of the L(1–169) protein expressed from within the Sindbis virus genome to deISGylate and deubiquitinate proteins by infecting BHK-21 cells (Figure 6B). Infection with 169GG or 169, but not MTGG or MT, reduced the amount of Ub conjugates detected in cells (Figure 6B, right panel), indicating that the viral OTU domain functions as a DUB enzyme when expressed from a Sindbis virus. Following transfection with ISG15 and its E1, E2, and E3 enzymes, ISGylated proteins can be detected in BHK-21 cells (Figure 6B, lane 1, middle panel). Infection with 169GG or 169 greatly reduced ISG15 conjugates, confirming that OTU expression results in deconjugation of ISGylated proteins. When cells were transfected with the E1, E2, and E3 enzymes but not ISG15, ISG15 conjugates were observed only following MTGG infection (Figure 6B, left panel). This shows that ISG15 expressed from dsTE12Q is capable of ISGylating proteins in the presence of the relevant conjugating enzymes but that this is only seen in the presence of a catalytically inactive form of the coexpressed L(1–169) protein (Figure 6B, lane 3, left panel).

We then determined whether OTU expression could counter ISG15's in vivo antiviral effect. In order to exclude effects due to IFNαβ-stimulated genes other than ISG15, we infected *IFNαβR*$^{-/-}$ mice (Figure 6C). Seventy percent of mice infected with a virus expressing ISG15 and the mutant OTU domain (MTGG) survived, consistent with previous observations that expression of ISG15 protects mice from lethality following Sindbis virus infection (Lenschow et al., 2005). In contrast, only 20% of mice infected with a virus expressing ISG15 and a functional OTU domain (169GG) survived infection ($p = 0.0015$). These data also correlate with our in vitro data demonstrating that L(1–169), but not L(1–169)2A, can deISGylate proteins following infection (Figure 6B). Mice infected with 169 or MT died with similar kinetics, demonstrating that the expression of L(1–169) did not increase the virulence of dsTE12Q in the absence of the IFN-mediated antiviral response. The slight increase in survival between 169GG and 169 ($p < 0.0001$) or MT ($p = 0.0032$) suggests that

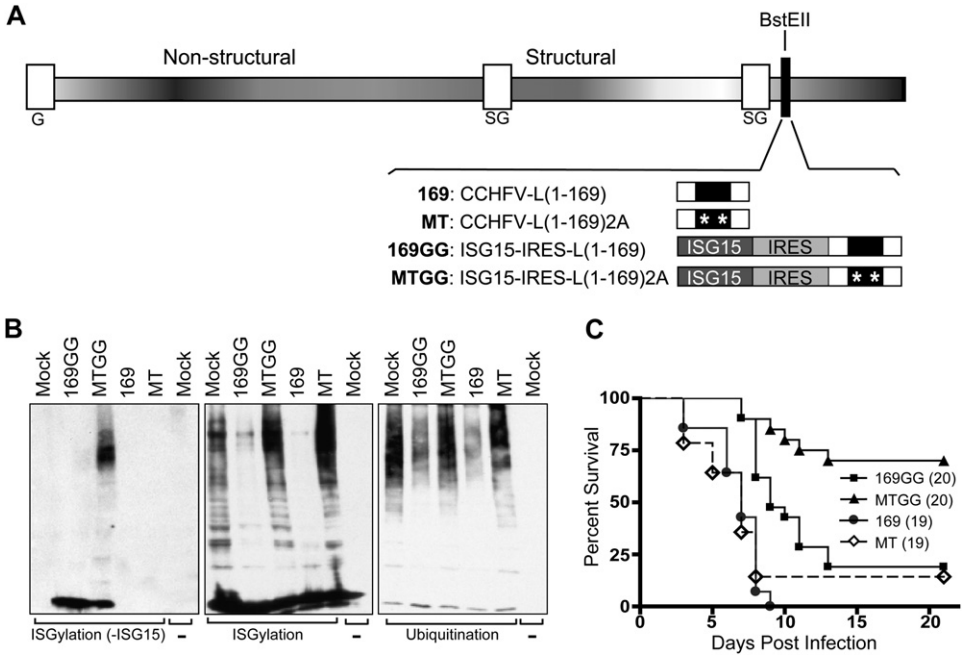

Figure 6. Sindbis Viruses Expressing the CCHFV-L OTU Domain Deconjugate Ub and ISG15 and Inhibit ISG15-Mediated Antiviral Effects in Mice

(A) Schematic diagram representing the CCHFV OTU domain-expressing Sindbis viruses utilized in these studies. G, genomic promoter; SG, subgenomic promoter.

(B) BHK-21 cells were transfected with UBE1L, UbcM8, and Herc5 (left panel), UBE1L, UbcM8, Herc5, and ISG15 (middle panel), or HA-Ub (right panel) and subsequently infected with recombinant Sindbis viruses as indicated. Cells lysates were immunoblotted with anti-ISG15 (left and middle panels) or anti-HA (right panel) antibodies. – indicates untransfected cells.

(C) *IFNαβR*$^{-/-}$ mice were infected with recombinant Sindbis viruses as indicated and monitored for survival. Data are pooled from four independent experiments, and numbers of mice in each group are indicated in parenthesis. Differences in survival were analyzed by the log-rank test: 169GG and 169 ($p < 0.0001$), 169GG and MT ($p = 0.0032$), 169GG and MTGG ($p = 0.0015$), MTGG and 169 ($p < 0.0001$), and MTGG and MT ($p < 0.0001$).

expression of the CCHFV OTU domain cannot completely antagonize the effects of ISG15 in this system. Nevertheless, these data show that expression of a catalytically active viral OTU domain can antagonize the antiviral effects of ISG15 in vivo.

Negative Regulation of the NF-κB Pathway by Viral OTU Domains

While the data above indicate that a viral OTU domain protease can counter the antiviral activities of ISG15, they do not address the possibility that the DUB activity of these proteins might also play a role in immune evasion. To address this hypothesis, we evaluated the effects of the CCHFV-L and EAV-nsp2 OTU domains on the NF-κB signaling pathway. Expression of the OTU domains of CCHFV-L and of EAV-nsp2 decreased in a dose-dependent manner the activation of an NF-κB-responsive promoter (Fujita et al., 1992) after TNFα treatment. This inhibition was similar to that mediated by A20, an OTU domain-containing inhibitor of the NF-κB pathway (Figure 7A). Inhibition was about 10-fold greater in the presence of the L(1–169) domain than the L(1–169)2A mutant, indicating a role for the OTU domain protease activity. These results were further confirmed by the ability of CCHFV-L(1–169) to inhibit NF-κB activation as measured by the inhibition of endogenous p65 nuclear translocation upon TNFα treatment (Figures 7B and 7C). The slight inhibition of NF-κB activation by the L(1–169)2A protein could be caused by some residual binding of this mutant to ubiquitinated substrates or by the presence of some other regulatory motifs within this protein. Nevertheless, the p65 nuclear translocation inhibition by the L(1–169) protein was significantly higher when compared to its mutant counterpart ($p = 0.0044$). Overall, these results demonstrate the ability of viral OTU domains to affect immune pathways that are regulated by ubiquitination.

DISCUSSION

Here we show that viral OTU domain-containing proteins are proteases that hydrolyze Ub and ISG15 from conjugated proteins. This dual deconjugating activity provide an elegant example of the economy of viral evolution, since both Ub and ISG15 rely on a conserved conjugation motif. Furthermore, the protease activity by the viral OTU domains has the physiologic capacity to evade two different cytokine pathways, IFNαβ and TNFα, that are fundamentally important for antiviral immunity.

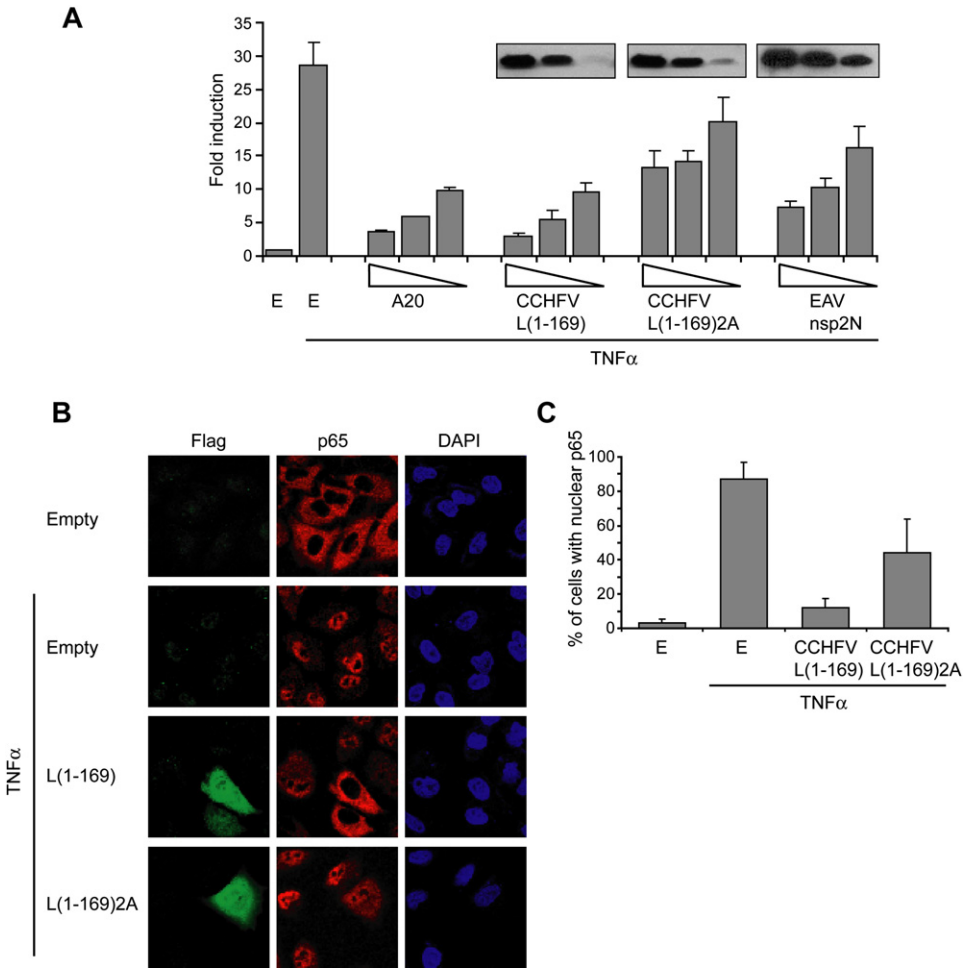

Figure 7. CCHFV-L and EAV-nsp2 OTU Domains Inhibit TNFα-Mediated NF-κB Activation

(A) NF-κB reporter assay in 293T cells transfected with OTU domains and treated with TNFα. Results shown are an average of three independent experiments. The western blot indicates expression of viral OTU proteins as detected with anti-HA [CCHFV-L(1–169) and CCHFV-L(1–169)2A] or anti-Flag antibodies (EAV-nsp2N). E, empty plasmid.

(B) A549 cells were transfected with indicated plasmids, stimulated with TNFα, and stained for p65 (red) and L(1–169) or L(1–169)2A (green). Nuclei were stained with DAPI (blue). The result shown is a representative of three independent experiments.

(C) L(1–169) or L(1–169)2A transfected cells in (B) were scored according to subcellular distribution of p65. Differences in p65 nuclear accumulation in TNFα-treated cells were analyzed by Student's t test: E and L(1–169) ($p < 0.0001$), E and L(1–169)2A ($p = 0.0007$), and L(1–169) and L(1–169)2A ($p = 0.0045$). E, empty plasmid. The result shown is a representative of three independent experiments.

Data in (A) and (C) are presented as mean ± SD (n = 3).

Viral DUB and DeISGylating Enzymes: A Unique Strategy for Immune Evasion?

Biochemical and genetic evidence supports the concept that protein ubiquitination plays a critical role in the induction of both the innate and the adaptive cellular immune system (Liu et al., 2005). For example, in addition to NF-κB signaling, Ub regulates several aspects of antiviral immunity, such as MHC class I and II antigen presentation (Loureiro and Ploegh, 2006; Shin et al., 2006), TLR/IL1 signaling (Chen, 2005), and induction of type I IFN by the cellular viral sensor RIGI (Gack et al., 2007). Inhibition of protein ubiquitination might also affect other cellular processes that can be subverted by viruses for their own advantage, such as the proteasome-mediated protein degradation system, multiple signal transduction events, or cell cycle progression. Given the effects that we observed on NF-κB signaling, it seems likely that viral OTU domain-containing proteases may be able to target these and other Ub-dependent pathways.

While the biochemical effects of ISGylation have been studied far less extensively than those of Ub, ISG15 is an important antiviral protein (Lenschow et al., 2005, 2007; Okumura et al., 2006). Thus, it is not surprising that viruses may use multiple strategies to counter the antiviral effects of ISG15. The work presented here provides a viral strategy for decreasing expression of bona fide ISG15 conjugates in cells. The first such strategy reported is the direct association of the NS1 protein of influenza B virus with ISG15. This association inhibits protein ISGylation by blocking the ISG15-UBE1L interaction (Yuan et al., 2002; Yuan

and Krug, 2001), while the viral OTU domain proteases analyzed here accomplish a similar effect via deconjugation.

The Ub and ISG15 deconjugation activities by the viral OTU domains contrast with the specific Ub deconjugation activity by the OTU domain-containing cellular proteins tested in this study. We speculate that other viral proteases, perhaps including some that do not have OTU domains, will be found to target both Ub- and ISG15-dependent processes. To date, viral DUB activities and in vitro cleavage of ISG15 fusion proteins have been demonstrated for the adenoviral protease adenain (Balakirev et al., 2002) and the papain-like proteases from the severe acute respiratory syndrome coronavirus (SARS-CoV) (Barretto et al., 2005; Lindner et al., 2005; Ratia et al., 2006).

OTU Domain Specificity and Deconjugating Activity, a Target for Antiviral Drug Development?

We found that the CCHFV-L OTU domain processed Ub and ISG15 conjugates and pro-ISG15 and pro-Nedd8 in vitro but did not have activity against any SUMO isoforms. Ub, ISG15, and Nedd8 differ from SUMO in their exposed C-terminal motifs: LRLRGG for Ub and ISG15 and LALRGG for Nedd8 versus QQQTGG for SUMO-2 and SUMO-3. This raises the interesting possibility that sequences similar to the LRLRGG motif may play an important role in substrate recognition and specific cleavage by CCHFV-L OTU and perhaps other viral proteases. Interestingly, the nsp2 of arteriviruses cleaves the nsp2/3 junction at FRLIGG (EAV) or GRLLGG (PRSSV) (Allende et al., 1999; Snijder et al., 1996; Ziebuhr et al., 2000), sequences similar to the LRLRGG motif. Thus, arterivirus OTU proteases have dual functions: performing essential viral polyprotein processing and targeting host substrates to modulate the antiviral response. This is analogous to the hepatitis C virus NS3-4A protease, which is involved both in viral polyprotein processing and in cleaving the cellular antiviral proteins TRIF and IPS-1 (Li et al., 2005; Lin et al., 2006).

The characterization of the CCHFV-L OTU domain and the development of in vitro assays for its enzymatic activities as described in this study will make it feasible to screen for potential inhibitors specific for CCHFV-L and other OTU domain-containing viral proteins. High-throughput screening of chemical compound libraries has proven to be a valuable tool in the identification of small-molecule inhibitors of other viral proteases such as HCV-NS3-4A (Sudo et al., 2005) and SARS-3CLpro (Blanchard et al., 2004). Since the viral OTU domains have a unique capacity to target both Ub and ISG15 conjugates, the design of specific inhibitors might be possible. For this reason, structural studies will be of great value to understand both the molecular basis of the unique biochemical activities of these viral proteins and the potential for development of antiviral compounds.

Physiologic Importance of Viral OTU Domain Protease DUB and DeISGylating Activities

Our demonstration that viral OTU domain-containing proteases can decrease both Ub and ISG15 conjugates in cells does not alone constitute proof that protease activity directed toward these substrates plays a role in viral infection. We were limited in performing the obvious experiment of assessing the role of viral OTU domain protease activity during infection by two things. First, CCHFV is a biosafety level 4 pathogen lacking a good animal model and whose molecular biology is not well enough developed to allow generation of mutant viruses. Second, the viral OTU domain proteases evaluated here either have, or are likely to have, important effects on processing of viral polyproteins (see above). Given this, we felt that it would be difficult to prove that these proteases have effects during infection that are solely attributable to their DUB and deISGylating activities. However, in transgenic mice, recombinant chimeric Sindbis viruses, and transfected cells, we found that viral OTU domain-containing proteases have significant effects on Ub- and ISG15-dependent host processes of known importance for innate immunity. We therefore conclude that these proteins have bona fide immune evasion properties. It will be interesting to further investigate the activities of these and other viral proteases that target Ub- and ISG15-dependent processes during viral infection.

EXPERIMENTAL PROCEDURES

Expression Plasmids

Plasmids pCAGGS-6HismISG15, pCAGGS-hUBE1L-HA, pFLAGCMV2-UbcM8, and pcDNA3.1-UbcM8 were provided by Dong-Er Zhang (Scripps Research Institute, La Jolla, CA) (Giannakopoulos et al., 2005). Herc5 was provided by Motoaki Ohtsubo (Kurume University, Fukuoka-ken, Japan). pcDNA 3.1^{+}-HA-Ub was provided by Dr. Domenico Tortorella (Mount Sinai School of Medicine, NY) (Treier et al., 1994). Peak10-Flag-A20 plasmid was provided by Dr. Adrian Ting (Mount Sinai School of Medicine). The construction of all other plasmids is described in the Supplemental Experimental Procedures.

Antibodies

Antibodies against Flag (M2 and rabbit polyclonal, Sigma, St. Louis, MO), HA (HA.7 [Sigma] HA.11 [Covance Research, Berkeley, CA]), Ub (P4D1, Cell Signaling, Danvers, MA,) NF-κB p65 (F-6, Santa Cruz Biotech, Santa Cruz, CA), and actin (AC-74, Sigma) were used following manufacturer's protocol. Anti-mouse ISG15 monoclonal (3C2 and 2D12) and polyclonal antibodies (Lenschow et al., 2005) and antiserum recognizing EAV-nsp2 (Snijder et al., 1994) have been previously described.

Purification of CCHFV L(1–169) from *E. coli*

BL-21 cells (Stratagene, La Jolla, CA) were transformed with pGEX-L(1–169) or pGEX-L(1–169)1A CCHFV, cultured to an OD_{600} of 0.6 in 2xYT medium and induced for 6 hr at 30°C with 0.1 mM IPTG. Bacteria were resuspended in lysis buffer (50 mM Tris-HCl, 5 mM EDTA, 1 mM DTT, 200 mM NaCl, and 0.1% NP-40), and purification of the GST fusion proteins was performed using GSH Sepharose resin (Amersham) according to the manufacturer's protocol. GST was cleaved using PreScission Protease (Pharmacia, Uppsala, Sweden) in cleavage buffer (50 mM Tris-HCl [pH 7.6], 150 mM NaCl, 1 mM EDTA, and 1 mM DTT).

Assays for DeISGylation in Cultured Cells

Initially, 293T cells cultured in 12-well dishes were cotransfected with 0.4 μg of pCAGGS-6HismISG15, 0.4 μg of pCAGGS-hUBE1L-HA, and 0.2 μg of pFLAGCMV2-UbcM8 along with OTU domain expression plasmids or empty pCAGGS plasmid using Lipofectamine 2000. In

subsequent experiments testing eukaryotic and viral OTU constructs, 293T cells in 12-well dishes were cotransfected with OTU domain expression plasmids and 0.5 μg pCAGGS-6His mISG15, 0.5 μg pCAGGS-mUBE1L-HA, 0.5 μg of plasmid encoding Herc5, and 0.2 μg pFLAGCMV2 UbcM8 or pCDNA3.1-UbcM8. Twenty-four hours posttransfection, cells were lysed in Laemmli sample buffer, boiled, and analyzed by immunoblot using anti-ISG15 mAb 3C2 as previously described (Lenschow et al., 2005). Each transfection experiment was performed a minimum of three times.

Assay for Deubiquitination in Cultured Cells

293T cells cultured in 12-well dishes were cotransfected with 0.5 μg of pcDNA3.1-HA-Ub and various OTU domain expression plasmids or empty pCAGGS plasmid using Lipofectamine 2000. Twenty-four hours posttransfection, the cells were lysed in Laemmli sample, boiled, and immunoblotted with anti-HA antibody. Each transfection experiment was performed a minimum of three times.

Generation of ISG15 Conjugates

Fourteen 10 cm dishes of 293T cells were transfected with 6 μg pCAGGS-6HismISG15, 3 μg pCAGGS-hUBE1L-HA, and 3 μg pFLAGCMV2-UbcM8. Twenty-four hours later, cells were harvested, resuspended in 20 mM Tris-HCl (pH 8.0) with 300 mM NaCl, and lysed by three cycles of freeze-thaw. Lysates were centrifuged for 15 min at 14,000 rpm. His-tagged ISG15 conjugates were purified over a His-Select Spin Column (SIGMA) following the manufacturer's directions. Column-bound conjugates were washed extensively with washing buffer (20 mM Tris-HCl [pH 8.0], 300 mM NaCl, and 5 mM Imidazole) and eluted with 20 mM Tris-HCl (pH 8.0), 300 mM NaCl, and 250 mM Imidazole. Protein concentration was measured by Bradford assay (Bio-Rad).

In Vitro Deconjugation Assays

K^{48} Ub_{2-7}, K^{63} Ub_{3-7}, SUMO-2_{2-8}, SUMO-3_{2-8}, pro-ISG15, pro-Nedd8, pro-SUMO-1, USP5/Isopeptidase T, NEDP1, UBP43, $A20_{CD}$, and His6-$SENP2_{CD}$ were purchased from Boston Biochem (Cambridge, MA). All reactions were performed in 50 mM Tris-HCl (pH 7.6), 5 mM MgCl2, and 2 mM DTT at 37°C for 2 hr. Serial 10-fold dilutions of L(1–169) or L(1–169)1A (ranging from 2.5 μM to 2.5 nM) were incubated with either 2.5 μg Ub chains or SUMO chains; 2.5 μg pro-ISG15, pro-Nedd8, or pro-SUMO-1; 10 μl *Ubp43*$^{-/-}$ lysate; or 3 μg of 6HisISG15 conjugates. Positive control for deconjugation was incubation with 100 mM USP5 (Ub), $SENP2_{CD}$ (SUMO), NEDP1 (Nedd8), or UBP43 (ISG15). Negative control was incubation of chains or conjugates in assay buffer alone. Reactions were terminated by addition of Laemmli sample buffer and separated by SDS-PAGE electrophoresis on a 4%–20% gradient gel (BioRad). Proteins were visualized by SimplyBlue Safestain (Invitrogen) staining (Ub and SUMO) or by anti-ISG15 western blot.

Viruses

Sindbis viruses were generated from a cDNA clone by in vitro transcription and RNA transfection of BHK-21 cells as previously described (Levine et al., 1996; Lenschow et al., 2005). Recombinant virus stocks were produced and titered on BHK-21 cells as previously described (Lenschow et al., 2005). Sindbis virus AR86 was a kind gift of Dr. Mark Heise (University of North Carolina, Chapel Hill) (Heise et al., 2000).

NF-κB Reporter Gene Assay

293T cells were cotransfected with 3.3-fold dilutions (starting at 100 ng) of A20, CCHFV-L(1–169), CCHFV-L(1–169)2A, EAV-nsp2N, or empty plasmid along with the firefly luciferase gene construct under the control of the NF-κB-binding sites) (Wang et al., 2000) and pRL-TK (*Renilla* luciferase; Promega, WI). The total amount of transfected DNA was kept constant by adding the pCAGGS empty vector. Twenty-four hours posttransfection, the cells were stimulated with TNFα (10 ng/ml) for 6 hr, and luciferase activities were measured using the Dual-Luciferase Reporter (DLR) Assay System (Promega). Final NF-κB luciferase values were normalized with the *Renilla* luciferase values as internal control.

Immunofluorescence

Two hundred nanograms of empty plasmid or Flag-tagged L(1–169) and L(1–169)2A were transfected into A549 cells. Twenty-four hours later, cells were stimulated with 10 ng/ml TNFα for 2 hr. Cells were fixed and permeabilized for 30 min at room temperature with 2.5% formaldehyde and 0.5% Triton X-100, washed extensively with PBS, and stained with anti-p65 and anti-Flag antibodies. Following PBS washes, cells were stained with anti-mouse (p65) or anti-rabbit (Flag) and secondary antibodies, and then mounted in medium containing an antifade reagent. Nuclear localization of p65 was scored in 100 to 400 transfected cells for each experimental condition.

Mouse Studies

IFNαβR$^{-/-}$ mice on the 129/SV/Pas background were initially obtained from M. Aguet, Swiss Institute of Experimental Cancer Research (Epalinges, Switzerland) (Behr et al., 2001; Dunn et al., 2005). CCHFV-L(1–1325) transgenic mice were generated at the WUSM Pathology Microinjection Core by microinjecting a linearized construct derived from pCAGGS-HA-L(1–1325) into B6 oocytes. Oocytes were implanted into pseudopregnant mice, and resulting litters were genotyped using PCR (primer sequences available upon request). Individual embryo MEFs from transgenic lines 1836, 1854, and 2929 were generated as described previously (Weck et al., 1999). Uninfected transgenic brain was homogenized in 1 ml of DMEM with protease inhibitors using 100 μl 1.0 mm diameter zirconia-silica beads in a MagNa Lyser (Roche, Indianapolis, IN). To assess transgene expression, 4 × 10^5 MEFs or 12 μl of brain homogenate were immunoblotted with HA.11 and anti-actin antibodies. Eight- to ten-week-old male *IFNαβR*$^{-/-}$ mice were infected subcutaneously (s.c.) in the left hind footpad with 5 × 10^6 PFU of virus diluted in 50 μl of Hank's balanced salt solution (HBSS). Four- to five-week old L(1–1325) transgenic mice were infected s.c. in the left hind footpad with 5000 PFU of Sindbis virus AR86 diluted in 50 μl of HBSS. Mice were bred and maintained at Washington University School of Medicine in accordance with all federal and university guidelines.

Statistical Analysis

All data were analyzed with Prism software (GraphPad, San Diego, CA). Survival data were analyzed by the log-rank (Mantel-Haenzsel) test, with death as the primary variable. Single-step growth curves were analyzed by one-way analysis of variance (ANOVA).

Supplemental Data

The Supplemental Data include Supplemental Experimental Procedures and two supplemental figures and can be found with this article online at http://www.cellhostandmicrobe.com/cgi/content/full/2/6/404/DC1/.

ACKNOWLEDGMENTS

We thank Richard Cadagan, Caroline Lai, and Lindsay Droit for technical assistance; Dr. Domenico Tortorella for helpful discussions; and Drs. Dong-Er Zhang, Motoaki Ohtsubo, Adrian Ting, and Dianne Griffin for providing reagents. This work was partially supported by DoD grants W81XWH-04-1-0876 and W81XWH-07-2-0028, and by a NIAID-funded Center to Investigate Virus Immunity and Antagonism (CIVIA) U19 AI62623 (to A.G.-S.), and by NIAID grants U54 AI057160 Projects 6 and 10 (to H.W.V.) and U54 AI057158 (to A.G.-S.).

Received: May 4, 2007
Revised: July 23, 2007
Accepted: September 21, 2007
Published: December 12, 2007

REFERENCES

Allende, R., Lewis, T.L., Lu, Z., Rock, D.L., Kutish, G.F., Ali, A., Doster, A.R., and Osorio, F.A. (1999). North American and European porcine reproductive and respiratory syndrome viruses differ in non-structural protein coding regions. J. Gen. Virol. *80*, 307–315.

Balakirev, M.Y., Jaquinod, M., Haas, A.L., and Chroboczek, J. (2002). Deubiquitinating function of adenovirus proteinase. J. Virol. *76*, 6323–6331.

Balakirev, M.Y., Tcherniuk, S.O., Jaquinod, M., and Chroboczek, J. (2003). Otubains: A new family of cysteine proteases in the ubiquitin pathway. EMBO Rep. *4*, 517–522.

Barretto, N., Jukneliene, D., Ratia, K., Chen, Z., Mesecar, A.D., and Baker, S.C. (2005). The papain-like protease of severe acute respiratory syndrome coronavirus has deubiquitinating activity. J. Virol. *79*, 15189–15198.

Behr, M., Schieferdecker, K., Buhr, P., Buter, M., Petsophonsakul, W., Sirirungsi, W., Redmann-Muller, I., Muller, U., Prempracha, N., and Jungwirth, C. (2001). Interferon-stimulated response element (ISRE)-binding protein complex DRAF1 is activated in Sindbis virus (HR)-infected cells. J. Interferon Cytokine Res. *21*, 981–990.

Blanchard, J.E., Elowe, N.H., Huitema, C., Fortin, P.D., Cechetto, J.D., Eltis, L.D., and Brown, E.D. (2004). High-throughput screening identifies inhibitors of the SARS coronavirus main proteinase. Chem. Biol. *11*, 1445–1453.

Boone, D.L., Turer, E.E., Lee, E.G., Ahmad, R.C., Wheeler, M.T., Tsui, C., Hurley, P., Chien, M., Chai, S., Hitotsumatsu, O., et al. (2004). The ubiquitin-modifying enzyme A20 is required for termination of Toll-like receptor responses. Nat. Immunol. *5*, 1052–1060.

Chen, Z.J. (2005). Ubiquitin signalling in the NF-κB pathway. Nat. Cell Biol. *7*, 758–765.

Dunn, G.P., Bruce, A.T., Sheehan, K.C., Shankaran, V., Uppaluri, R., Bui, J.D., Diamond, M.S., Koebel, C.M., Arthur, C., White, J.M., and Schreiber, R.D. (2005). A critical function for type I interferons in cancer immunoediting. Nat. Immunol. *6*, 722–729.

Evans, P.C., Smith, T.S., Lai, M.J., Williams, M.G., Burke, D.F., Heyninck, K., Kreike, M.M., Beyaert, R., Blundell, T.L., and Kilshaw, P.J. (2003). A novel type of deubiquitinating enzyme. J. Biol. Chem. *278*, 23180–23186.

Evans, P.C., Ovaa, H., Hamon, M., Kilshaw, P.J., Hamm, S., Bauer, S., Ploegh, H.L., and Smith, T.S. (2004). Zinc-finger protein A20, a regulator of inflammation and cell survival, has de-ubiquitinating activity. Biochem. J. *378*, 727–734.

Fujita, T., Nolan, G.P., Ghosh, S., and Baltimore, D. (1992). Independent modes of transcriptional activation by the p50 and p65 subunits of NF-κB. Genes Dev. *6*, 775–787.

Gack, M.U., Shin, Y.C., Joo, C.H., Urano, T., Liang, C., Sun, L., Takeuchi, O., Akira, S., Chen, Z., Inoue, S., and Jung, J.U. (2007). TRIM25 RING-finger E3 ubiquitin ligase is essential for RIG-I-mediated antiviral activity. Nature *446*, 916–920.

Giannakopoulos, N.V., Luo, J.K., Papov, V., Zou, W., Lenschow, D.J., Jacobs, B.S., Borden, E.C., Li, J., Virgin, H.W., and Zhang, D.E. (2005). Proteomic identification of proteins conjugated to ISG15 in mouse and human cells. Biochem. Biophys. Res. Commun. *336*, 496–506.

Haas, A.L., Ahrens, P., Bright, P.M., and Ankel, H. (1987). Interferon induces a 15-kilodalton protein exhibiting marked homology to ubiquitin. J. Biol. Chem. *262*, 11315–11323.

Heise, M.T., Simpson, D.A., and Johnston, R.E. (2000). A single amino acid change in nsP1 attenuates neurovirulence of the Sindbis-group alphavirus S.A.AR86. J. Virol. *74*, 4207–4213.

Honig, J.E., Osborne, J.C., and Nichol, S.T. (2004). Crimean-Congo hemorrhagic fever virus genome L RNA segment and encoded protein. Virology *321*, 29–35.

Karin, M., and Ben-Neriah, Y. (2000). Phosphorylation meets ubiquitination: The control of NF-κB activity. Annu. Rev. Immunol. *18*, 621–663.

Kim, K.I., Giannakopoulos, N.V., Virgin, H.W., and Zhang, D.E. (2004). Interferon-inducible ubiquitin E2, Ubc8, is a conjugating enzyme for protein ISGylation. Mol. Cell. Biol. *24*, 9592–9600.

Kinsella, E., Martin, S.G., Grolla, A., Czub, M., Feldmann, H., and Flick, R. (2004). Sequence determination of the Crimean-Congo hemorrhagic fever virus L segment. Virology *321*, 23–28.

Kirkin, V., and Dikic, I. (2007). Role of ubiquitin- and Ubl-binding proteins in cell signaling. Curr. Opin. Cell Biol. *19*, 199–205.

Lenschow, D.J., Giannakopoulos, N.V., Gunn, L.J., Johnston, C., O'Guin, A.K., Schmidt, R.E., Levine, B., and Virgin, H.W., IV. (2005). Identification of interferon-stimulated gene 15 as an antiviral molecule during Sindbis virus infection in vivo. J. Virol. *79*, 13974–13983.

Lenschow, D.J., Lai, C., Frias-Staheli, N., Giannakopoulos, N.V., Lutz, A., Wolff, T., Osiak, A., Levine, B., Schmidt, R.E., Garcia-Sastre, A., et al. (2007). IFN-stimulated gene 15 functions as a critical antiviral molecule against influenza, herpes, and Sindbis viruses. Proc. Natl. Acad. Sci. USA *104*, 1371–1376.

Levine, B., Goldman, J.E., Jiang, H.H., Griffin, D.E., and Hardwick, J.M. (1996). Bc1-2 protects mice against fatal alphavirus encephalitis. Proc. Natl. Acad. Sci. USA *93*, 4810–4815.

Li, K., Foy, E., Ferreon, J.C., Nakamura, M., Ferreon, A.C., Ikeda, M., Ray, S.C., Gale, M., Jr., and Lemon, S.M. (2005). Immune evasion by hepatitis C virus NS3/4A protease-mediated cleavage of the Toll-like receptor 3 adaptor protein TRIF. Proc. Natl. Acad. Sci. USA *102*, 2992–2997.

Lin, R., Lacoste, J., Nakhaei, P., Sun, Q., Yang, L., Paz, S., Wilkinson, P., Julkunen, I., Vitour, D., Meurs, E., and Hiscott, J. (2006). Dissociation of a MAVS/IPS-1/VISA/Cardif-IKKepsilon molecular complex from the mitochondrial outer membrane by hepatitis C virus NS3-4A proteolytic cleavage. J. Virol. *80*, 6072–6083.

Lindner, H.A., Fotouhi-Ardakani, N., Lytvyn, V., Lachance, P., Sulea, T., and Menard, R. (2005). The papain-like protease from the severe acute respiratory syndrome coronavirus is a deubiquitinating enzyme. J. Virol. *79*, 15199–15208.

Liu, Y.C., Penninger, J., and Karin, M. (2005). Immunity by ubiquitylation: A reversible process of modification. Nat. Rev. Immunol. *5*, 941–952.

Loeb, K.R., and Haas, A.L. (1992). The interferon-inducible 15-kDa ubiquitin homolog conjugates to intracellular proteins. J. Biol. Chem. *267*, 7806–7813.

Loureiro, J., and Ploegh, H.L. (2006). Antigen presentation and the ubiquitin-proteasome system in host-pathogen interactions. Adv. Immunol. *92*, 225–305.

Makarova, K.S., Aravind, L., and Koonin, E.V. (2000). A novel superfamily of predicted cysteine proteases from eukaryotes, viruses and Chlamydia pneumoniae. Trends Biochem. Sci. *25*, 50–52.

Malakhov, M.P., Kim, K.I., Malakhova, O.A., Jacobs, B.S., Borden, E.C., and Zhang, D.E. (2003). High-throughput immunoblotting. Ubiquitiin-like protein ISG15 modifies key regulators of signal transduction. J. Biol. Chem. *278*, 16608–16613.

Nanao, M.H., Tcherniuk, S.O., Chroboczek, J., Dideberg, O., Dessen, A., and Balakirev, M.Y. (2004). Crystal structure of human otubain 2. EMBO Rep. *5*, 783–788.

Narasimhan, J., Potter, J.L., and Haas, A.L. (1996). Conjugation of the 15-kDa interferon-induced ubiquitin homolog is distinct from that of ubiquitin. J. Biol. Chem. *271*, 324–330.

Nijman, S.M., Luna-Vargas, M.P., Velds, A., Brummelkamp, T.R., Dirac, A.M., Sixma, T.K., and Bernards, R. (2005). A genomic and functional inventory of deubiquitinating enzymes. Cell *123*, 773–786.

Okumura, A., Lu, G., Pitha-Rowe, I., and Pitha, P.M. (2006). Innate antiviral response targets HIV-1 release by the induction of ubiquitin-like protein ISG15. Proc. Natl. Acad. Sci. USA *103*, 1440–1445.

Ratia, K., Saikatendu, K.S., Santarsiero, B.D., Barretto, N., Baker, S.C., Stevens, R.C., and Mesecar, A.D. (2006). Severe acute respiratory syndrome coronavirus papain-like protease: Structure of a viral deubiquitinating enzyme. Proc. Natl. Acad. Sci. USA *103*, 5717–5722.

Shin, J.S., Ebersold, M., Pypaert, M., Delamarre, L., Hartley, A., and Mellman, I. (2006). Surface expression of MHC class II in dendritic cells is controlled by regulated ubiquitination. Nature *444*, 115–118.

Snijder, E.J., Wassenaar, A.L., and Spaan, W.J. (1994). Proteolytic processing of the replicase ORF1a protein of equine arteritis virus. J. Virol. *68*, 5755–5764.

Snijder, E.J., Wassenaar, A.L., Spaan, W.J., and Gorbalenya, A.E. (1995). The arterivirus Nsp2 protease. An unusual cysteine protease with primary structure similarities to both papain-like and chymotrypsin-like proteases. J. Biol. Chem. *270*, 16671–16676.

Snijder, E.J., Wassenaar, A.L., van Dinten, L.C., Spaan, W.J., and Gorbalenya, A.E. (1996). The arterivirus nsp4 protease is the prototype of a novel group of chymotrypsin-like enzymes, the 3C-like serine proteases. J. Biol. Chem. *271*, 4864–4871.

Sudo, K., Yamaji, K., Kawamura, K., Nishijima, T., Kojima, N., Aibe, K., Shimotohno, K., and Shimizu, Y. (2005). High-throughput screening of low molecular weight NS3-NS4A protease inhibitors using a fluorescence resonance energy transfer substrate. Antivir. Chem. Chemother. *16*, 385–392.

Tergaonkar, V. (2006). NFκB pathway: A good signaling paradigm and therapeutic target. Int. J. Biochem. Cell Biol. *38*, 1647–1653.

Treier, M., Staszewski, L.M., and Bohmann, D. (1994). Ubiquitin-dependent c-Jun degradation in vivo is mediated by the delta domain. Cell *78*, 787–798.

Wang, X., Li, M., Zheng, H., Muster, T., Palese, P., Beg, A.A., and Garcia-Sastre, A. (2000). Influenza A virus NS1 protein prevents activation of NF-κB and induction of alpha/beta interferon. J. Virol. *74*, 11566–11573.

Wang, Y., Satoh, A., Warren, G., and Meyer, H.H. (2004). VCIP135 acts as a deubiquitinating enzyme during p97-p47-mediated reassembly of mitotic Golgi fragments. J. Cell Biol. *164*, 973–978.

Weck, K.E., Kim, S.S., Virgin, H.I., and Speck, S.H. (1999). B cells regulate murine gammaherpesvirus 68 latency. J. Virol. *73*, 4651–4661.

Wertz, I.E., O'Rourke, K.M., Zhou, H., Eby, M., Aravind, L., Seshagiri, S., Wu, P., Wiesmann, C., Baker, R., Boone, D.L., et al. (2004). De-ubiquitination and ubiquitin ligase domains of A20 downregulate NF-κB signalling. Nature *430*, 694–699.

Whitehouse, C.A. (2004). Crimean-Congo hemorrhagic fever. Antiviral Res. *64*, 145–160.

Yuan, W., and Krug, R.M. (2001). Influenza B virus NS1 protein inhibits conjugation of the interferon (IFN)-induced ubiquitin-like ISG15 protein. EMBO J. *20*, 362–371.

Yuan, W., Aramini, J.M., Montelione, G.T., and Krug, R.M. (2002). Structural basis for ubiquitin-like ISG 15 protein binding to the NS1 protein of influenza B virus: A protein-protein interaction function that is not shared by the corresponding N-terminal domain of the NS1 protein of influenza A virus. Virology *304*, 291–301.

Zhao, C., Beaudenon, S.L., Kelley, M.L., Waddell, M.B., Yuan, W., Schulman, B.A., Huibregtse, J.M., and Krug, R.M. (2004). The UbcH8 ubiquitin E2 enzyme is also the E2 enzyme for ISG15, an IFN-alpha/beta-induced ubiquitin-like protein. Proc. Natl. Acad. Sci. USA *101*, 7578–7582.

Ziebuhr, J., Snijder, E.J., and Gorbalenya, A.E. (2000). Virus-encoded proteinases and proteolytic processing in the Nidovirales. J. Gen. Virol. *81*, 853–879.